

# STUDY OF ALUMINIUM AND ALUMINIUM-ZINC ALLOYS AT LOW TEMPERATURES BY ULTRASONIC PULSE-ECHO TECHNIQUE

By

JAYANTA BANDYOPADHYAY

ME  
1975  
D  
BAN  
STU

TH  
HE/1975/D  
B 2235



DEPARTMENT OF METALLURGICAL ENGINEERING

INDIAN INSTITUTE OF TECHNOLOGY KANPUR

AUGUST 1975

# **STUDY OF ALUMINIUM AND ALUMINIUM-ZINC ALLOYS AT LOW TEMPERATURES BY ULTRASONIC PULSE-ECHO TECHNIQUE**


**A Thesis Submitted  
in partial Fulfilment of the Requirements  
for the Degree of  
DOCTOR OF PHILOSOPHY**

**By  
JAYANTA BANDYOPADHYAY**

**to the**

**DEPARTMENT OF METALLURGICAL ENGINEERING  
INDIAN INSTITUTE OF TECHNOLOGY KANPUR  
AUGUST 1975**

I.I.T. KANPUR  
CENTRAL LIBRARY

 A 46608

19 JUL 1976

ME-1975-D-BAN-STU

## CERTIFICATE

Certified that the work presented in this thesis has been carried out under my supervision and that the work has not been submitted elsewhere for a degree.

August, 1975

( K.P. Gupta )  
Professor  
Department of Metallurgical Engg.,  
Indian Institute of Technology, Kanpur,  
INDIA



## ACKNOWLEDGEMENT

Acknowledgement to specific individuals is rather a difficult task for me, since during the long course of the work extremely valuable help and suggestions came from a large number of friends and coworkers, and in the very beginning I solicit excuse for any omission.

I am thankful to Prof. K.P. Gupta for suggesting the problem, making the equipments available and participating at all stages of the work. My discussions with Dr. R.N. Biswas and Dr. P.K. Chatterjee of the Electrical Engineering Department proved useful in the modifications of the electronic equipments used. I am grateful to Dr. S.K. Sinha, Dr. S.K. Ghatak and Dr. A. Ramakrishna of the Saha Institute of Nuclear Physics for sharing their experiences in the same field.

The excellent machining of Mr. K.R. Sharma of the Advanced Centre for Electronic Systems, I.I.T. Kanpur was a great help in the construction of the equipments. The cooperation from the employees of I.I.T. Kanpur, particularly those of the Central Workshop, Central Instrumentation Service, Precision Workshop, the Low Temp. Laboratory and the laboratories of the Metallurgical Engineering Department is thankfully remembered.

Contributions in material and labour came ceaselessly from my friends Dr. S.K. Si, Mr. M.V. Raja, Mr. T.V.S. Ramanujan, Dr. A.K. Hui, Dr. S.K. Ray, Mr. P.S.S. Sarma, Mr. K.P. Mukherjee, Mr. C.B. Chaudhary, Dr. S.D. Phatak, Mr. G.C. Baral and many others. My fiancée, Miss Vandana Shiva's consistent participation during the writing accelerated the completion of the thesis to a great extent. I thank all of them.

The author is thankful to Mr. C.M. Abraham for making a quick and neat typescript of the text.

JAYANTA BANDYOPADHYAY

## CONTENTS

Chapter		Page
	LIST OF TABLES	vii
	LIST OF FIGURES	xi
	SYNOPSIS	xiii
1.1.	INTRODUCTION	1
1.1	The Debye Temperature	3
1.2	Debye Temperature and Crystal Elastic Moduli	5
1.3	Methods of Integration	9
1.4	Debye Temperature and Isotropic Sound Velocities	10
1.5	Methods of Measurement of Elastic Constants	16
1.6	Statement of the Problem	21
2.	THE ULTRASONIC PULSE - ECHO EQUIPMENT	23
2.1	The Specimen Holding Assembly	27
2.2	Electronic Systems	31
2.3	Operation and Performance of the Pulse - Echo Equipment	34
3.	X-RAY DIFFRACTOMETER ATTACHMENT FOR LOW TEMPERATURES	39
3.1	The Liquid Nitrogen Tank	43
3.2	The Base of the Attachment	44
3.3	Operation and Performance of the Low Temperature Attachment	47

Chapter	Page
4.	60
EXPERIMENTAL PROCEDURE	
4.1	60
Preparation of Specimens	
4.2	66
Procedure for Operation of the Ultrasonic Equipment with High Zn Alloys	
4.3	67
Procedure for Operation of the X-Ray Attach- ment with High Zn Alloys	
4.4	68
Calibration of Thermocouples	
5.	70
RESULTS	
6.	101
DISCUSSION	
7.	115
CONCLUSIONS	
	117
	REFERENCE
APPENDIX	123
Detailed Procedure for the Operation of the Ultrasonic Equipment	

## LIST OF TABLES

Table	Page
1. Propagation direction for pure shear and longitudinal waves and the velocity in terms of the elastic moduli	8
2. Values of $\rho$ computed from the same single crystal moduli by VRH method and the digital computer	13
3. Elastic moduli of single crystal and polycrystalline Tungsten at 280°K	15
4. Instruments used in the electrical circuits	26
5. Longitudinal wave velocity in copper	38
6. The peak positions and lattice parameters of Aluminium as obtained at 306°K by using the spectrogoniometer specimen holder and low temperature attachment	52
7. Observed lattice parameters of Aluminium at different temperatures	56
8. Low temperature lattice parameters of Al calculated on the basis of van Arp's thermal contraction data published by NBS	59
9. Tentative and analysed composition of the alloys	64
10. The observed e.m.f. values for the thermocouples at the calibration points	69
11. Measured longitudinal wave velocity in Aluminium	73
12. Measured shear wave velocity in Aluminium	73
13. Measured longitudinal wave velocity in Aluminium 1 percent Zn alloys	74
14. Measured shear wave velocity in Aluminium 1 percent Zn alloy	74

Table	Page
15. Measured longitudinal wave velocity in Aluminium 2 percent Zn alloy	75
16. Measured shear wave velocity in Aluminium 2 percent Zn alloy	75
17. Measured longitudinal wave velocity in Aluminium 3 percent Zn alloy	76
18. Measured shear wave velocity in Aluminium 3 percent Zn alloy	76
19. Measured longitudinal wave velocity in Aluminium 4 percent Zn alloy	77
20. Measured shear wave velocity in Aluminium 4 percent Zn alloy	77
21. Measured longitudinal wave velocity in Aluminium 10 percent Zn alloy	78
22. Measured shear wave velocity in Aluminium 10 percent Zn alloy	78
23. Measured longitudinal wave velocity in Aluminium 15 percent Zn alloy	79
24. Measured shear wave velocity in Aluminium 15 percent Zn alloy	79
25. Measured lattice parameter of Aluminium 1 percent Zn alloy	80
26. Measured lattice parameter of Aluminium 2 percent Zn alloy	80
27. Measured lattice parameter of Aluminium 3 percent Zn alloy	81
28. Measured lattice parameter of Aluminium 4 percent Zn alloy	81
29. Measured lattice parameter of Aluminium 10 percent Zn alloy	82
30. Measured lattice parameter of Aluminium 15 percent Zn alloy	82

Table		Page
31.	Instrumental errors entering in the results	83
32.	Bulk modulus, shear modulus, Young's modulus, coefficient of Thermal Expansion and Debye temperature of Aluminium determined through the least square fit of the measured data	84
33.	Bulk modulus, shear modulus, Young's modulus coefficient of thermal expansion and Debye temperature of Aluminium 1 percent Zn alloy determined through least square fit of the measured data	85
34.	Bulk modulus, shear modulus, Young's modulus coefficient of thermal expansion and Debye temperature of Aluminium 2 percent Zn alloy determined through least square fit of the measured data	86
35.	Bulk modulus, shear modulus, Young's modulus coefficient of thermal expansion and Debye temperature of Aluminium 3 percent Zn alloy determined through least square fit of the measured data	87
36.	Bulk modulus, shear modulus, Young's modulus coefficient of thermal expansion and Debye temperature of Aluminium 4 percent Zn alloy determined through least square fit of the measured data	88
37.	Bulk modulus, shear modulus, Young's modulus coefficient of thermal expansion and Debye temperature of Aluminium 10 percent Zn alloy determined through least square fit of the measured data	89
38.	Bulk modulus, shear modulus, Young's modulus coefficient of thermal expansion and Debye temperature of Aluminium 15 percent Zn alloy determined through least square fit of the measured data	90

T. Table	Page
39. Lattice parameter of Aluminium from various sources	106
40. Debye temperature of some Al-Zn alloys calculated from measured values	109
41. Debye temperature of Al from various sources	110



## LIST OF FIGURES

Figure		Page
1.	Bulk modulus of $\alpha$ Cu-Al alloys	18
2.	Shear modulus of $\alpha$ Cu-Al alloys	18
3.	Block diagram for the pulse-echo equipment	25
4.	The specimen holding assembly for the pulse-echo equipment	29
5.	A photograph of the pulse-echo equipment	35
6.	Longitudinal wave echo train in Aluminium at room temperature	35
7.	Block diagram for the low temperature attachment	40
8.	The low temperature attachment for X-ray diffractometer	42
9.	A photograph of the low temperature attachment	46
10.	The (420) reflection for Al at two temperatures showing $\alpha_1$ and $\alpha_2$ peaks	51
11.	Lattice parameter of Al at room temperature obtained with two specimen holders	54
12.	Measured lattice parameter of Al at low temperatures and calculated lattice parameters on the basis of room temperature lattice parameter and thermal contraction data of van Arp et al published by NBS	58
13.	The Al-rich side of the Al-Zn constitution diagram	62
14.	Temperature dependence of the longitudinal wave velocity in Al and Al-Zn alloys	92

Figure	Page
15. Temperature dependence of the shear wave velocity in Al and Al-Zn alloys	94
16. Temperature dependence of the lattice parameter of Al-Zn alloys	96
17. Debye temperature of Al and Al-Zn alloys	98
18. Variation of the $0^\circ\text{K } \Theta_D$ bulk modulus and shear modulus as a function of atomic percent Zn	100

## SYNOPSIS

STUDY OF ALUMINIUM AND ALUMINIUM - ZINC ALLOYS AT LOW TEMPERATURE  
BY ULTRASONIC PULSE - ECHO TECHNIQUE

A Thesis Submitted  
In Partial Fulfilment of the Requirements  
For the Ph.D. Degree

by  
JAYANTA BANDYOPADHYAY  
to the

Department of Metallurgical Engineering  
Indian Institute of Technology, Kanpur  
August, 1975

An ultrasonic pulse - echo equipment for the measurement of ultrasonic wave velocity in solids between  $1.4^{\circ}\text{K}$  and room temperature was set up. The performance of the pulse - echo equipment was tested at  $77^{\circ}\text{K}$  and  $306^{\circ}\text{K}$  using a 99.99 pct. pure polycrystalline copper specimen. The observed velocity of 10 MHz longitudinal waves in copper at these two temperatures was found to be 4881 M/sec and 4762 M/sec respectively and were in good agreement with the average velocity of longitudinal ultrasonic waves calculated from the published single crystal elastic moduli of copper.

For the determination of lattice parameter at low temperatures an attachment for a General Electric XRD - V X-ray diffractometer was also constructed. The performance of the attachment at room temperature was compared with that of a standard specimen holder supplied with the diffractometer. For both the cases the lattice parameter of 99.9 pct. pure aluminium at

306°K was found to be  $4.0489 \overset{\circ}{\text{\AA}}$  by using a least square extrapolation against  $\cos^2\theta$ . The measured lattice parameter of Al at 306°K was in good agreement with the published lattice parameter data of Al. The lattice parameter corresponding to the (420) reflection was found to be the same, within the experimental error limit, as of the extrapolated values. Hence, only this reflection was used for the determination of lattice parameter at different temperatures. The lattice parameter of Al was found at intermediate temperatures between 89°K and 306°K. The variation of the lattice parameter with temperature also agreed well with that calculated using the thermal contraction data of aluminium obtained by different experimental techniques.

Lattice parameters and velocities of longitudinal and shear waves in polycrystals of Al and six binary Al-Zn alloys (with 1.2, 3, 4, 10 and 15 at.pct.Zn) were measured from above 77°K. The alloys were in the quenched solid solution state and without any clustering effect. Measurements were made between 77°K and 306°K for specimens with Zinc content upto 4 at.pct. For two alloys with high Zn content (10 and 15 at.pct.Zn) measurements upto about 225°K could be taken, since close to room temperature clustering and zone formation is known to occur.

To obtain the velocity and the lattice parameter for the temperature range 0°K to 300°K, the measured parameters were fitted

with a fourth order polynomial in temperature by the least square method. The precondition for the polynomial was a monotonic change in slope of the parameter vs temperature curve and the slope would tend to zero as temperature approached  $0^{\circ}\text{K}$ . The polynomials were used to calculate the thermal expansion coefficient, bulk moduli, shear moduli and Young's moduli and the Debye temperature ( $\Theta_D$ ) of the alloys at  $25^{\circ}\text{K}$  interval between  $0^{\circ}\text{K}$  and  $300^{\circ}\text{K}$ . Derived values of these parameters for Al at room temperature ( $300^{\circ}\text{K}$ ) were found to be  $23.2 \times 10^{-6}/^{\circ}\text{K}$ , 748 Kbar, 256 Kbar, 690 Kbar and  $402^{\circ}\text{K}$  respectively.  $\Theta_D$  for Al at  $0^{\circ}\text{K}$  was found to be  $421^{\circ}\text{K}$ .

The good agreement between the present data and the published data shows that the use of polycrystalline specimens for the estimation of  $\Theta_D$  is a reasonable alternative of the single crystal method.

The variation with temperature of the two velocities and the lattice parameters of Al-Zn alloys resemble that of pure Al. The variation of  $\Theta_D$  and shear modulus with Zn content show a continuous decrease while in case of bulk modulus a maxima occurs near 10 at.pct.Zn and no regular variation was found.

The change in  $\Theta_D$  with increasing solute content could not be clearly and quantitatively interpreted due to paucity of single crystal data on a few Al alloy systems. A simplified and qualitative analysis of the decrease in  $\Theta_D$  has been made. The

increase in the average atomic mass, decrease in the lattice parameter and the Young's modulus might be the reasons behind the reduction in  $\theta_D$ .

## CHAPTER 1

### INTRODUCTION

Low temperature specific heat measurement is a very important and widely used experimental method for the study of band structure of solids. The specific heat of materials is measured by noting the rise in temperature due to the absorption of a small amount of supplied heat. The total specific heat thus obtained is the sum total of many different contributions. For the simplest case, the specific heat at constant volume consists of two terms

$$C_v = [C_v]_{\text{electronic}} + [C_v]_{\text{lattice}} \quad (1)$$

At low temperatures, particularly at liquid helium temperatures the two contributions become comparable in magnitude. The electronic specific heat, which is proportional to the absolute temperature, is expressed as  $\gamma T$ , where  $\gamma$  is proportional to the density of states at the Fermi surface at  $T = 0^\circ\text{K}$  [ $N(E_F(0))$ ]. The lattice specific heat, according to the Debye theory, is proportional to the cube of absolute temperature and is expressed as  $\beta T^3$ , where  $\beta$  is another constant. The term  $\beta$  is related to a parameter called Debye temperature  $\theta_D$ , through the following relation,

$$\beta = \frac{12 \pi^4}{5} \frac{N k}{\Theta_D^3} = \frac{233.78 Nk}{\Theta_D^3} \quad (2)$$

Since the Debye temperature for most materials is not known, the usual practice is to get  $\gamma$  and  $\beta$  by a least square fit of the specific heat data with the equation

$$C_v = \gamma T + \beta T^3 \quad (3)$$

The above method of finding  $\gamma$ , however, does not always lead to very accurate values. As for example in the case of some Cr-Fe-Al alloys Pessal, Gupta, Cheng, and Beck<sup>1</sup> reported equally good least square fit of specific heat data with widely varying values of  $\beta$ . To determine the density of states at the Fermi level with sufficient accuracy, over and above the specific heat data, an independent measurement of the Debye temperature is necessary. It is possible to relate  $\Theta_D$  with the elastic moduli of solids. The measurement of elastic moduli thus can be used to determine independently the Debye temperature and hence lattice specific heat at liquid He temperatures. In the following sections the Debye temperature  $\Theta_D$ , the relation of  $\Theta_D$  with the elastic moduli of solids and the methods of determination of the elastic moduli have been reviewed.



### 1.1 The Debye Temperature:

As the temperature is increased from absolute zero, the measured specific heat of crystalline materials increases rapidly from zero (at  $T = 0^{\circ}\text{K}$ ) and approaches a value of about 6 cal/mole/deg at sufficiently high temperatures. Einstien<sup>2</sup> first proposed that the specific heat is due to thermal vibration of atoms. He assumed that all atoms vibrate independent of each other and with the same frequency. Using these assumptions Einstein obtained the general nature of the specific heat versus temperature curve, but his specific heat versus temperature curve approached zero more rapidly than actually observed. Born and von Karman<sup>3</sup> and Debye<sup>4</sup> almost simultaneously realised that the atoms can not vibrate independent of each other and as a result there can not be a single frequency of vibration but a frequency spectrum. Born and von Karman treated the solid as an association of mass-centres connected and held together by generalised springs at all distances. In the case of three dimensional lattice approach the problem of trying to find the frequency spectrum with the help of the force constants, whose characteristics were not clearly understood, was however, quite difficult.

In Debye's<sup>4</sup> approach the solid was assumed to be a continuum, with a vibrational spectrum whose frequency distribution was shown to be proportional to  $\nu^2$  and with a cut off at  $\nu_D$  (Born<sup>5</sup> also has shown that for long wavelengths the frequency spectrum is proportional to  $\nu^2$ ) such that the total number of degrees of freedom was limited to  $3N$ ,  $N$  being the total number of discrete mass points in the solid. Debye considered standing waves in a cube of length  $L$  and volume  $V$  and the cube could possess many standing waves ranging in frequency from zero upto the cut-off frequency  $\nu_D$ . Debye also assumed that the velocity of sound waves observed in a crystal at radio frequencies would hold approximately upto  $\nu_D$ . In a real solid, there are three different types of sound waves, one longitudinal and two transverse waves, associated with each crystallographic direction of propagation and the total number of frequencies is actually the sum of the contributions from each type of wave averaged over all directions of propagation. The total number of degrees of freedom is then given by

$$3N = \int_0^{\nu_D} N(\nu) d\nu = \frac{4}{3} \pi V \nu_D^3 \int_{\text{all directions}} \left[ \frac{1}{v_1^3} + \frac{1}{v_2^3} + \frac{1}{v_3^3} \right] \frac{d\Omega}{4\pi} \quad (4)$$

where  $N(\nu)$  is the density of states at frequency  $\nu$ ,  $v_1, v_2, v_3$  are the three velocities and  $d\Omega$  is the

solid angle element corresponding to the three velocities. Since  $\Theta_D$  is defined as  $\frac{h v_D}{k}$ , therefore, Eqn. (4) gives

$$\Theta_D = \frac{h v_D}{k} = \frac{h}{k} \left( \frac{9 N}{4 \pi V} \right)^{1/3} \left\{ \left[ \frac{1}{v_1^3} + \frac{1}{v_2^3} + \frac{1}{v_3^3} \right] \int_{\text{all directions}} \frac{d\Omega}{4\pi} \right\}^{-1/3} \quad (5)$$

With the help of Eqns. (4) and (5), Debye calculated the lattice specific heat which in the low temperature limit of  $T < \Theta_D/50$  is given by

$$C_v = \frac{12 \pi^4}{5} Nk \left( \frac{T}{\Theta_D} \right)^3 \quad (6)$$

## 1.2 Debye Temperature and Crystal Elastic Moduli:

At sufficiently low temperatures the Debye approximation in Eqn. (6) holds and at these temperatures only the long wavelength acoustic waves are excited. Such acoustic waves are in the magacyle region and the velocities can be used for the determination of the Debye temperature. Sound velocity data at such low temperatures are scanty but extrapolation of relatively higher temperature data to absolute zero can be made for comparison purposes without much error<sup>5</sup>.

The theoretical basis for the independent estimation of  $\Theta_D$  lies in the relationship of  $\Theta_D$  with sound velo-

cities (Eqn. 5) and  $\Theta_D$  can be found if solution to the integral in Eqn. 5 can be found. For the solution of the integral, the relationship between velocity of sound waves in a material and its elastic constants is made use of. This relationship is available through Musgrave's work<sup>6</sup>. Using the generalised Hook's law, the equation of motion of an element anywhere inside the volume and the propagation of plane waves in directions defined by the direction cosines  $l, m$  and  $n$  Musgrave<sup>6</sup> showed that the three sound wave velocities would be the three roots of a secular equation defined by

$$\begin{vmatrix} A - \rho v^2 & \alpha\beta & \gamma\alpha \\ \alpha\beta & \beta - \rho v^2 & \beta\gamma \\ \gamma\alpha & \beta\gamma & C - \rho v^2 \end{vmatrix} = 0 \quad (7)$$

where  $v$  is the velocity,  $\rho$  is the density,  $A, B, C, \beta\gamma, \gamma\alpha$  and  $\alpha\beta$  are functions of the direction cosines and the single-crystal elastic moduli defined as

$$A = l^2 C_{11} + m^2 C_{66} + n^2 C_{55} + 2mn C_{56} + 2nl C_{15} + 2lm C_{16} \quad (8)$$

$$B = l^2 C_{66} + m^2 C_{22} + n^2 C_{44} + 2mn C_{24} + 2nl C_{46} + 2lm C_{26} \quad (9)$$

$$C = l^2 C_{55} + m^2 C_{44} + n^2 C_{33} + 2mn C_{34} + 2nl C_{35} + 2lm C_{45} \quad (10)$$

$$\alpha\beta = l^2 C_{16} + m^2 C_{26} + n^2 C_{45} + mn(C_{46} + C_{25}) + nl(C_{14} + C_{56}) + lm(C_{12} + C_{66}) \quad (11)$$

$$\beta\gamma = l^2 C_{15} + m^2 C_{46} + n^2 C_{35} + mn(C_{45} + C_{36}) + nl(C_{13} + C_{55}) + lm(C_{14} + C_{56}) \quad (12)$$

$$\gamma\alpha = l^2 C_{56} + m^2 C_{24} + n^2 C_{34} + mn(C_{44} + C_{25}) + nl(C_{36} + C_{45}) + lm(C_{25} + C_{46}) \quad (13)$$

Using Musgrave's expressions, the integration of equation (5) over the whole angular range becomes possible if the single crystal elastic moduli are known. The Musgrave relations simplify considerably when the more symmetric crystal classes are considered. As for example in the case of cubic crystals there are only 3 independent elastic moduli  $C_{11}$ ,  $C_{12}$  and  $C_{44}$ . These moduli are related to the various sound wave velocities in the crystal lattices and could be easily determined by measuring the velocities for suitable propagation directions of pure longitudinal or transverse waves. Along any general direction of propagation it is not possible to get a pure longitudinal

Table 1 : Propagation Directions for pure shear and longitudinal waves and the velocities in terms of the elastic moduli.

Direction of propagation	Direction of displacement	type of wave	Velocity <sup>+</sup>
[100]	[100]	Longitudinal	$[C_{11}/\rho]^{\frac{1}{2}}$
[100]	[010]	Shear	$[C_{44}/\rho]^{\frac{1}{2}}$
[100]	[001]	Shear	"
[110]	[110]	Longitudinal	$[\frac{C_{11}+C_{12}+2C_{44}}{\rho}]^{\frac{1}{2}}$
[110]	[001]	Shear	$[C_{44}/\rho]^{\frac{1}{2}}$
[110]	[010]	Shear	$[\frac{C_{11}-C_{12}}{\rho}]^{\frac{1}{2}}$

<sup>+</sup>  $\rho$  is density

or shear mode. Table I gives the crystallographic directions in which pure shear and longitudinal wave can be obtained in a cubic crystal<sup>7</sup>.

### 1.3 Methods of Integration

With the success of Musgrave in the replacement of the three sound velocities by the direction cosines of the propagation direction and the elastic moduli the only effective step to be taken towards an independent method for the estimation of Debye temperature was to evaluate the integral in expression (5). The complexity of the relations between  $l, m, n, C_{11}, C_{12}$  etc and the velocities made the use of high-speed computers the only suitable method for solving the integral. Alers<sup>8</sup> has developed a computer program for the determination of  $\Theta_D$  which estimates  $\Theta_D$  value with an accuracy better than 0.1 pct.

A number of indirect methods have also been developed and they have reasonable accuracies. The simplest and most widely used method is due to deLaunay<sup>9</sup>. DeLaunay considered a cubic lattice of the Born and Von Karman type with central force connecting nearest and next nearest neighbour atoms and took into account the compressibility of the electron gas to arrive at Debye temperature given by

$$\Theta_D^3 = \frac{9N}{4\pi V} \left( \frac{h}{K} \right)^3 \left( \frac{C_{44}}{\rho} \right)^{3/2} \frac{9}{18 + \sqrt{3}} f(S, t) \quad (14)$$

where  $f(S, t)$  is a function of the anisotropy,  $S$  and  $t$  are the functions of the elastic moduli  $C_{11}, C_{12}$  and  $C_{44}$ .

He made tables for finding  $f(S, t)$  for values of  $S$  and  $t$  which could be determined from the measured value of  $C_{11}$ ,  $C_{12}$  and  $C_{44}$ . In the case of copper, this method produced results within  $0.01^\circ\text{K}$  of the  $\Theta_D$  computed by electronic computer method. Graphical method of Marcus<sup>10</sup>, power series expansion of Hopf and Lechner<sup>11</sup> and Quimby and Sutton<sup>12</sup> yielded  $\Theta_D$  values correct to a tenth of a percent. Harmonic series expansion method has been used by Bhatia and Tauber<sup>13</sup> and Betts et al<sup>14</sup> and agreement within 0.25 percent of the computer results were obtained. Using Fedorov's<sup>15</sup> general theory in invariant form for the propagation of plane elastic waves in homogeneous crystalline solids Fedorov and Bystrova developed approximation methods. Konti and Varshni<sup>17</sup> used this method for cubic elements and found general agreement with the results obtained from the Hopf and Lechner<sup>11</sup> and Bhatia and Tauber<sup>13</sup> methods.

#### 1.4 Debye Temperature and Isotropic Sound Velocities

For a perfectly isotropic crystal the sound velocities are independent of crystallographic directions and in terms of the only two velocities  $v_l$  and  $v_s$ , the longitudinal and shear velocities respectively, the Debye temperature is given simply by

$$\Theta_D = \frac{h}{k} \left( \frac{9N}{4\pi v} \right)^{1/3} \left( \frac{1}{v_l^3} + \frac{2}{v_s^3} \right)^{-1/3} \quad (15)$$



or

$$\Theta_D = \frac{h}{k} \left( \frac{3N}{4\pi v} \right)^{1/3} v_m \quad (16)$$

where  $v_m$  is called the mean velocity defined by

$v_m = \left[ \frac{1}{3} \left( \frac{1}{v_l^3} + \frac{2}{v_s^3} \right) \right]^{-1/3}$ . For isotropic case  $v_l$  and  $v_s$  are related to the bulk and shear moduli  $K$  and  $G$  through the relations

$$v_l = \left[ \frac{1}{\rho} \left( K + \frac{4}{3} G \right) \right]^{1/2} \quad (17)$$

$$v_s = \left[ \frac{G}{\rho} \right]^{1/2} \quad (18)$$

Almost all crystals are an-isotropic and so the Eqn. (15) can not be applied for single crystals. A polycrystalline material with randomly oriented equiaxed grains will, however, behave like a truly isotropic material and a relation similar to Eqn. 15 should be applicable.

There have been systematic approaches by Voigt<sup>18</sup>, Reuss<sup>19</sup>, Hill<sup>20</sup> and Gilvarey<sup>21</sup> to the problem of finding relations between the single crystal elastic moduli and the polycrystalline elastic moduli,  $K$  and  $G$ . Hill has shown that neither Voigt nor Reuss equations yield the correct polycrystalline  $K$  and  $G$  from the single crystal elastic moduli, and indicated that Voigt and Ruess values actually are the upper and lower limits, respectively. Hill

suggested that an arithmetic mean of Voigt and Reuss K and G will give the correct polycrystalline bulk and shear moduli, that is :

$$K_H = \frac{K_V + K_R}{2} \quad (19)$$

$$G_H = \frac{G_V + G_R}{2} \quad (20)$$

where suffixes H, V and R represent Hill, Voigt and Reuss respectively.

Anderson<sup>22</sup> has shown that if the VRH model is chosen then two average velocities can be defined as

$$\bar{v}_1 = \left[ \frac{1}{\rho} (K_H + \frac{4}{3} G_H) \right]^{\frac{1}{2}} \quad (21)$$

$$\bar{v}_s = \left( \frac{G_H}{\rho} \right)^{\frac{1}{2}} \quad (22)$$

and in terms of these velocities the average velocity  $\bar{v}_m$  is given by

$$\bar{v}_m = \left[ \frac{1}{3} \left( \frac{1}{\bar{v}_1^3} + \frac{2}{\bar{v}_s^3} \right) \right]^{-1/3} \quad (23)$$

In a polycrystalline material the measured velocities are averaged over all directions due to randomness of the grains. Anderson<sup>22</sup> compared the  $\Theta_D$  values of various materials calculated from single crystal elastic

Table 2 : Values of  $\theta_D$  computed from the same single crystal moduli by the VRH method and the digital computer.

Material	$\theta_{VRH} (^{\circ}K)$	$\theta_{Computer} (^{\circ}K)$
Ag	226.5	226.4
Al	426.2	426.6
Au	161.7	161.6
Cu	344.5	345.3
Li	326.0	325.9
Ni	476.2	476.2
Th	164.2	164.2
V	393.2	394.0
Beryl	1463.5	1462.0
Cd	214.0	213.0
Mg	386.0	385.8
Zn	328.3	328.1

moduli by the VRH model and the rigorous computation techniques (Table II).

The close correspondence of  $\Theta_D$  values of Table II indicates that the integral in Eqn. (5) can be replaced by the average sound velocity  $\bar{v}_m$ . Since in a polycrystalline material the averaging of sound velocity over all directions is automatically achieved due to the randomness of the grains, longitudinal and shear velocities measured in a polycrystalline material will be the same as  $\bar{v}_l$  and  $\bar{v}_s$ . Hence, Eqn. 15 can be used for  $\Theta_D$  determination with  $v_l$  and  $v_s$  replaced by  $\bar{v}_l$  and  $\bar{v}_s$  or  $\bar{v}_m$  replaced with  $\bar{v}_m$ .

The experimental verification of the similarity of the Debye temperature obtained by using single crystals and polycrystals have also been made. Anderson<sup>22</sup> showed that the extrapolated values of the experimentally observed bulk elastic properties of dense sintered Alumina (no porosity) is very close to the mean value proposed by Hill. The case of the elastic moduli of single and polycrystalline tungsten is interesting. Because of isotropy of tungsten  $C_{11}$  and  $C_{44}$  for single crystals are expected to be same as the  $\rho v_l^2$  (longitudinal modulus) and  $\rho v_s^2$  (shear modulus) for the polycrystals.

Table 3 : Elastic moduli of single and polycrystalline Pungsten at 280°K<sup>23,24</sup>

$C_{11}$ Kbar	Long.mod. K bar <sup>2</sup> ( $f \cdot v_1$ )	$C_{44}$ K bar	Sh.Mod. K bar ( $f v_s^2$ )	$\bar{v}_1$ (Single) M/sec	$v_1$ (Poly) M/sec	$\bar{v}_s$ (single) M/sec	$v_s$ (Poly) M/sec
5245	5189	1609	1569	5201	5198	2870	2864

Elastic moduli of single crystal of Tungsten has been reported by Featherstone and Neighbours<sup>23</sup> and that of a polycrystal has been reported by Bernstein<sup>24</sup>. For comparison both data are shown in Table III.

The equivalence of the bulk properties observed with polycrystalline samples and calculated on the basis of single crystal data can also be seen for a few alloy systems. The results of the studies on polycrystalline elastic constants of Cu-Al alloys at room temperature by Lenkhery and Lahteenkorva<sup>25</sup> match well with the value of the constants calculated from the single crystal data of Cain and Thomas<sup>26</sup> and Moment<sup>27</sup>. The comparison is shown in Figs. 1 and 2. Room temperature studies on both single and poly crystals of Al-Zn alloys has been made by Rokhlin<sup>28,29</sup> and the satisfactory equivalence has been established. Thus it appears that where moderately accurate  $\Theta_D$  values are necessary, the polycrystalline elastic constants may be conveniently used.

### 1.5 Methods of the Measurement of Elastic Constants

The various methods used for the measurement of elastic constants of both single and polycrystalline specimens may be classified as static, dynamic and scattering methods. Voigt<sup>30</sup> introduced the static methods as early as 1928. The static methods are no more favoured in recent times due to the greatly enhanced accuracy and simplicity of



**Fig. 1 Bulk modulus of  $\alpha$  Cu-Al alloys**

Reference	25	•
Reference	26	▼
Reference	27	△

**Fig. 2 Shear modulus of  $\delta\alpha$  Cu-Al alloys**

Reference	25	•
Reference	26	▼
Reference	27	△



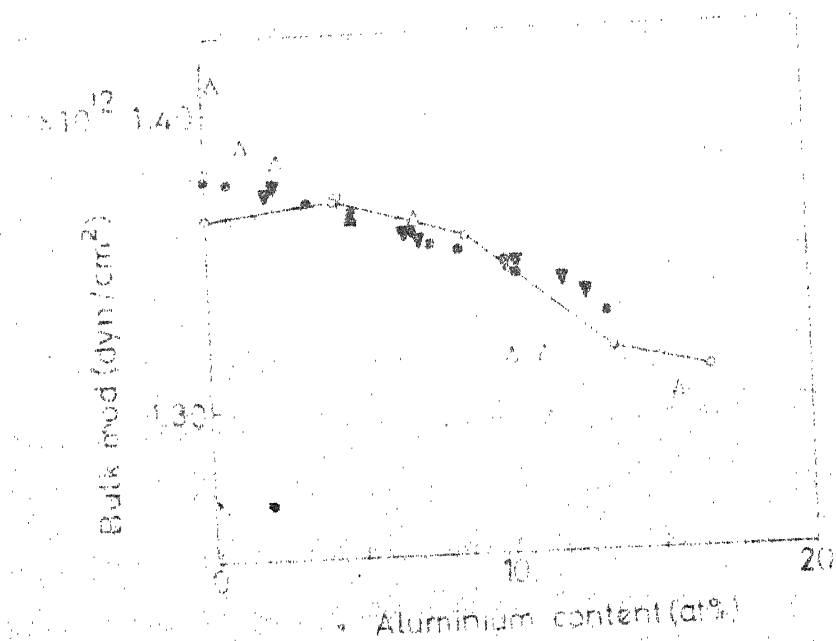


Fig. 1

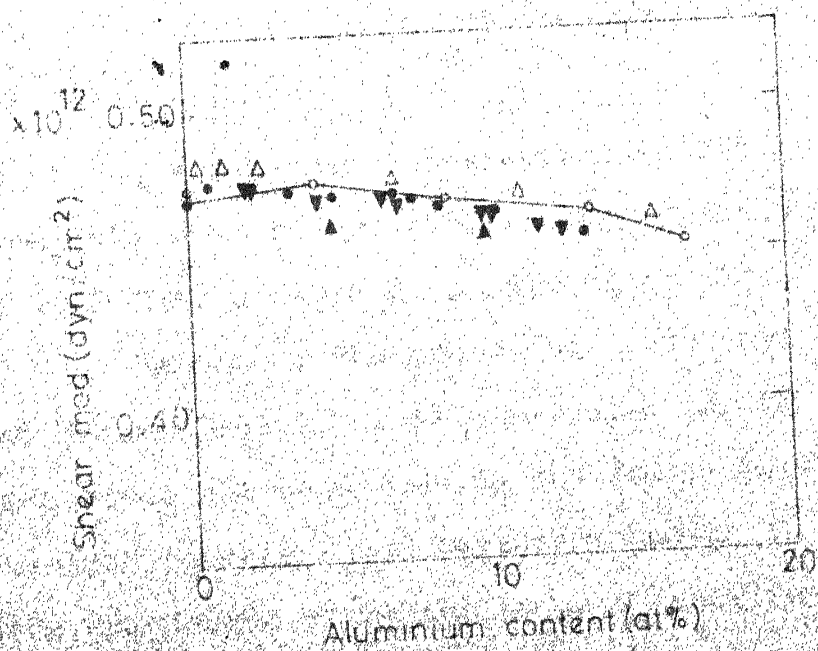


Fig. 2

the dynamic methods, Fine<sup>31</sup> gives a systematic review of the dynamic methods which he divides into two groups. The first group is characterized by the use of lower frequency ( $<1$  MHz) ultrasonic waves for the establishment of standing waves in a system involving the specimen. The resonance period and the physical dimensions are used to find the velocity, Numerous methods have been used to excite mechanical resonance, Electromagnetic fields have been used for ferromagnetic materials<sup>32</sup>, and electrostatic probes for non-magnetic materials<sup>33,34</sup>. Piezoelectric discs cemented to the specimen under study is a common tool for exciting mechanical vibrations. In India an ultrasonic wedge method, developed by Bhagavantam<sup>35</sup> has found wide application.

With the development of electronics and radar techniques, the use of high-powered high-frequency ( $>1$  MHz to about 1000 MHz) ultrasonic pulses finds wide application<sup>36-39</sup>. Resonance technique has been used by Bolef and Menen<sup>40</sup> but the most widespread use of the ultrasonic waves has been made in the Pulse-Echo technique. The pulse-echo technique has been very useful in studies of elastic properties of materials as a function of temp. and pressure. In this technique, a quartz plate transducer is cemented to one of the two parallel faces of the specimen and a pulse of the order of a microsecond

is generated and allowed to echo back and forth. From the time delay between successive echoes, the velocity is measured and the elastic moduli determined. This technique has attracted the attention of various workers and consequently, many modifications came into existence. With a relatively simple circuit Viswanathan<sup>41</sup> has shown that the accuracy of velocity measurement can be increased to 0.5 percent. A phase-comparison method has been used by Mason and Bommel<sup>42</sup> and it has been further improved by Blume<sup>43</sup>. Another phase-comparison method has been developed by McSkimin<sup>44</sup>. Continuous wave resonance method of Bolef and deLlerk<sup>45</sup> has an accuracy of 0.1 ppm. Pulse superposition method developed by McSkimin<sup>44</sup> has an accuracy of a few parts in  $10^4$ , whereas his phase-comparison method has an accuracy of 1 part in  $10^4$ .

Several other methods have also been used for measurement of elastic constants of materials. Electromagnetic waves have been used in a limited manner for the determination of elastic constants. Brillouin's<sup>46</sup> fine structure analysis method has been used by Chandrasekhar<sup>47</sup> and Flubacher<sup>48</sup>. Another method which involves the measurement of the intensity of the thermal diffuse scattering of X-Rays and neutrons has also proved useful<sup>49,50</sup>. In general, however, the scattering techniques are not as simple and as accurate as the dynamic methods.

## 1.6 Statement of the Problem

In the preceding sections it has been shown that the Debye temperature of solids can be determined with reasonable accuracy from the average sound velocity obtained by measuring the velocities of longitudinal and shear waves in a polycrystalline sample. These sound velocities also give quite accurate values of the various polycrystalline elastic moduli. For the estimation of Debye temperature an additional data in the form of number of atoms per unit volume is also necessary. If the crystal structure is known for a material, number of atoms/unit volume can be found easily by measuring lattice parameter as a function of temperature. The thermal expansion coefficients of materials can also be obtained from the measurement of lattice parameter. Thus from the measurement of two types of sound velocities and the lattice parameter a wide range of physical properties of a material can be determined simultaneously.

Of the several methods of sound velocity measurement in solids the pulse-echo technique is the most accurate and the measurement technique is also simple. In this investigation this method has been employed. A pulse echo technique equipment was assembled and the necessary specimen holder assembly was designed, the details of which will be found in Chapter 2.

Of the several methods available for determining volume as a function of temperature, the one considered simplest and very accurate is the lattice parameter method. For accurate lattice parameter measurement a GE diffractometer was chosen. A low temperature attachment for the diffractometer was designed and fabricated, the details of which are given in Chapter 3.

Of the various alloy systems the Al-base alloys are chosen because of two reasons. The attenuation of ultrasonic waves in Al-base alloys is about one order of magnitude less than in other common alloy systems. The low attenuation would give rise to larger number of observable echoes in the echo-train, thus ensuring higher accuracy of measurement. The Al-Zn system is particularly chosen because of the wide application of Al-Zn alloys as sound conductors<sup>51,52</sup>.

No Debye temperature/is available for these data/  
alloys. In this investigation Debye temperature, and the elastic moduli of Al-Zn alloys have been determined as a function of Zn content and temperature.

## CHAPTER 2

### THE ULTRASONIC PULSE-ECHO EQUIPMENT

Debye temperature  $\Theta_D$  of solids is proportional to the mean velocity of sound,  $v_m$  (Eqn. 16). The mean velocity can be determined through the measurement of velocities of longitudinal and transverse ultrasonic waves in suitably oriented single crystals or in polycrystalline samples. To determine  $\Theta_D$  at  $0^\circ\text{K}$  sound velocities in solids are measured as a function of temperature and  $\Theta_D$  at  $0^\circ\text{K}$  is determined with the help of velocities extrapolated to  $0^\circ\text{K}$ . The extrapolation of velocities to  $0^\circ\text{K}$  can be done from relatively higher temperatures, such as liquid  $\text{N}_2$  temperature, or the measurements may be extended to liquid He temperatures. Even though for the present work the sound velocity measurements were carried out between liquid  $\text{N}_2$  temperature and  $300^\circ\text{K}$ , keeping the whole range of temperatures in mind the ultrasonic pulse-echo apparatus was designed to work between  $4.2^\circ\text{K}$  and room temperature.

The wide temperature range of determining sound velocities in solids can be conveniently divided into two regions -  $4.2^\circ$  to  $77^\circ\text{K}$  and  $77^\circ$  to  $300^\circ\text{K}$ , attainable by using liquid He and liquid  $\text{N}_2$  respectively. Compared to operating the pulse - echo equipment between  $4.2^\circ\text{K}$  and

300°K, the loss of liquid He is expected to be much smaller when operated between 4.2° and 77°K. A further cut in the requirement of liquid He can be made by using the equipment like an adiabatic calorimeter in which the specimen is first brought to liquid He temperature by bringing the specimen in thermal contact with the He bath through an exchange gas and then isolating it from the surroundings by creating high vacuum in the specimen chamber. In this method a small heater will be able to heat the specimen to any desired temperature between 4.2 and 77°K and only a small amount of liquid He will be required, since none or a very small amount of heat from the elevated temperature specimen will flow out to the liquid He bath. For the higher temperature region the specimen may be held at different heights above liquid N<sub>2</sub> kept in a tall dewar and thus any desired temperature may be obtained. In the present design these features were kept in mind.

The block diagram for the pulse - echo equipment used in the present investigation is shown in Fig. 3 and the list of instruments used is given in Table 4. The pulse - echo equipment essentially consists of two basic parts, a) the specimen holding assembly with the facility for varying the specimen temperature and b) electronic

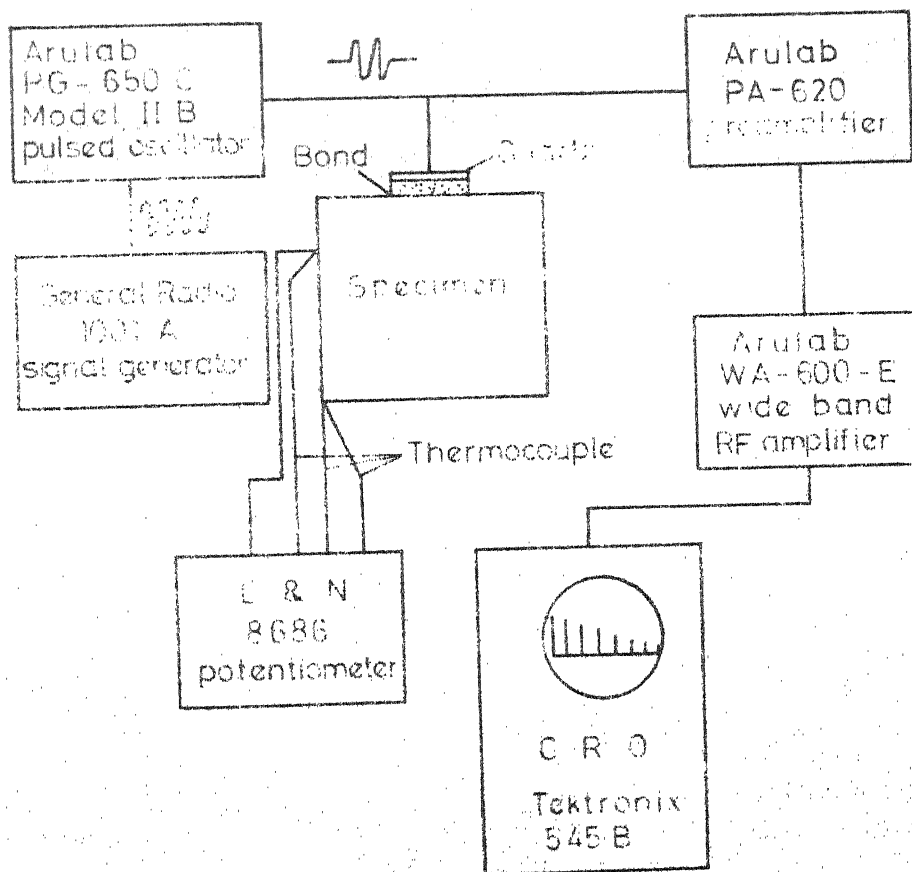


Fig. 3 Block diagram for the pulse-echo equipment.



Table 4 : Instruments used in the Electrical Circuits

Instrument	Specification	Manufacturer
Standard Signal Generator Model GR 1001 - A	Range: 5 KHz to 50 MHz Accuracy: $\pm 1$ percent of reading	General Radio Company, U. S. A.
High Powered Pulsed Oscillator PG-650-C Model II with Add 2A	Range: 5-97 MHz Accuracy: $\pm 10$ KHz	Aronberg Ultra- sonic Lab. Inc. U. S. A.
Wide Band Amplifier with Preamplifier Model WA-600-E, and PA-620	Amplification range: 0-85 db	" "
Cathode Ray Oscillos- cope with L-Type plug-in-unit Model: 545 B	Range: dc to 30 MHz (Dual Time Base)	Tektronix, Inc., U. S. A.
Potentiometer Cat.No. 8686	Range: 0 to 100 mV Accuracy: $\pm 0.005$ mv	Leeds and North- rup Co., U. S. A.

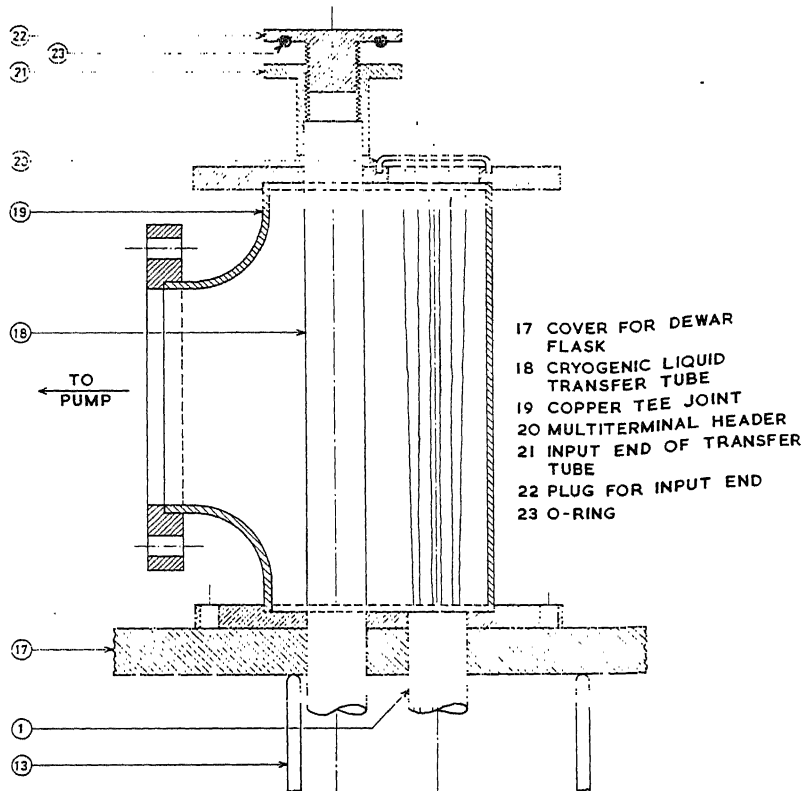
equipments for the generation and detection of ultrasonic pulses. The details of each of these parts of the pulse - echo equipment is given in the following sections.

## 2.1 The Specimen Holding Assembly

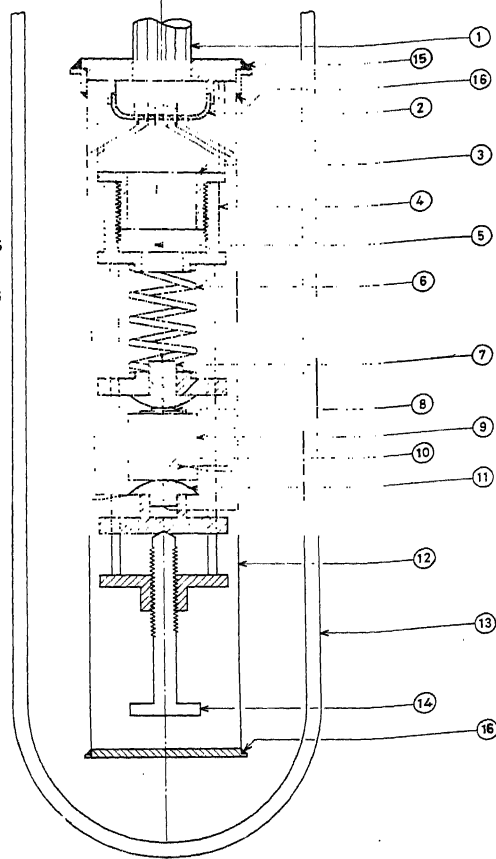
The specimen holding assembly, which is shown in Fig. 4 has essentially three parts - the specimen holder to keep good mechanical contact between the transducer and the specimen, a can to make an adiabatic chamber for the specimen, and a metal head to fit on a He cryostat. The specimen holding assembly was designed to fit the He cryostat set up by Si et al<sup>53</sup>. The can, 1.25" in diameter and 7" long, was made of a thin wall stainless steel tube (12). It was closed at the bottom by silver brazing a thin copper plate to it. The open end of the can was silver brazed to a thin copper ring which could be snugly put on a cylindrical copper block attached to a 30" long and 0.5" diameter thin walled stainless steel tube. To make a leak proof joint the can was soldered to the cylindrical copper block with Wood's metal (15).

A threaded copper support for the specimen holder assembly was attached to the cylindrical copper block (at the end of the 30" long stainless steel tube) through three short stainless steel rods. The specimen holder assembly consisted of an internally threaded cylindrical teflon

**Fig. 4 The specimen holding assembly for the pulse - echo equipment**



- 1 THINWALL STAINLESS TUBE FOR SPECIMEN HOLDER
- 2 MULTITERMINAL HEADER
- 3 COPPER SUPPORT FOR TEFLON SPECIMEN HOLDER
- 4 TEFLON SPECIMEN HOLDERS
- 5 R. F. INPUT CONNECTION
- 6 COPPER-BERYLLIUM SPRING
- 7 CONTACT FOR TRANSDUCER
- 8 TRANSDUCER
- 9 SPECIMEN
- 10 THERMOCOUPLES
- 11 SUPPORT AND EARTH POINT FOR SPECIMEN
- 12 STAINLESS TUBE CAN
- 13 CRYOGENIC LIQUID DEWAR
- 14 ADJUSTING SCREW
- 15 WOODS METAL JOINT
- 16 SILVER BRAZING



piece which rigidly supported three stainless steel guide rods and a threaded teflon bottom piece. A teflon adjusting screw (14) was used through the bottom piece to facilitate raising or lowering of the specimen. Two teflon pieces, which could move freely along the guide rods and fitted with two rounded copper electrical contact points were used to hold the specimen (9). The quartz transducer (8), gold plated on one side, was put on the top surface of the specimen and the bottom copper contact point was used for ground connection (11). In order to have proper contact between the specimen, transducer and the electrical contact points a Cu-Be spring (6) was used between the teflon support and the top sliding teflon piece. The adjusting screw (14) was used to adjust the pressure of the copper contacts on the transducer.

Two 36 gauge Copper - Constantan thermocouples (10) were used to measure the specimen temperature. For working below liquid  $N_2$  temperature a small heater made of insulated 40 gauge manganin wire wound round a copper block could be fixed on the specimen to raise the specimen temperature. All the eight electrical connections were led out of the specimen holder through a multiterminal Kovar plug. The Kovar plug was also used to provide a thermal shield for the specimen chamber. The lead wires were taken

out of the specimen chamber through the Kovar plug and the  $\frac{1}{2}$ " dia stainless steel tube and was terminated on another multiterminal Kovar plug fixed at the top of the metal head. The wires inside the  $\frac{1}{2}$ " dia tube were insulated by using 26 gauge teflon spaghetti.

The metal head consisted of a 2" dia copper Tee which was fitted with two brass flanges on two ends and was closed at the third end, by a brass cap. The Kovar plug was soldered to this brass cap. The 30" long stainless steel tube was silver brazed to the brass flange opposite to the closed end. A  $\frac{1}{2}$ " dia stainless steel tube fitted with an O-ring screw cap was also inserted through the brass cap and the flange to provide an opening for introducing a liquid He transfer line. The second flanged opening was provided for connecting the specimen holder assembly to a high vacuum system consisting of a 140 lit/min capacity mechanical pump, a 2" dia Veeco diffusion pump, a liquid N<sub>2</sub> trap and Veeco thermocouple and ionisation gauges.

## 2.2 Electronic Systems

The pulse - echo technique utilizes electrical pulses of suitable length and frequency to activate some electro-mechanical transducers, like the X,Y or AC cut quartz transducers. The transducers are bonded to one of the two parallel plane surfaces of the specimen. For the present work

X and Y cut quartz transducers were used to generate longitudinal and transverse waves. The resonant frequency of both types of transducers was 10 MHz. The electrical signals to be fed to the transducer was generated by a general Radio 1001-A Standard Signal Generator. The continuous wave was shaped to pulses of  $1\frac{1}{2}$   $\mu$ sec length and 2.5 KHz prf by an ARULAB PG-650-C Model II High Powered Pulsed Oscillator used as a Gated Amplifier. The output frequency of the Signal Generator was kept fixed at 10 MHz, the resonant frequency of the quartz transducer used in this investigation.

Since only one transducer was used to excite the original pulses and to sense the echoes, the signals corresponding to the echoes were available at the same terminal (Fig. 3). The echo pulses were very weak and were amplified in two stages. An ARULAB PA-620-B preamplifier was used to get a preliminary gain of about 20 to 25 db. The preamplifier was tuned to the carrier wave frequency and the optimum amplification without distortion of the pulses was achieved by adjusting the various amplification gains at the input and output stages of the preamplifier. The output of the preamplifier was then fed to an ARULAB WA-600-E wideband amplifier for amplification with a gain of about 70 to 80 db. The video output of the wide

band amplifier consisted of the positive envelopes of the echo pulses and the main pulse. The video output was displayed on a Tektronix 545 B Oscilloscope with Type L plug-in-unit.

The Tektronix 545 B Oscilloscope had two time bases, A and B. In the present investigation A delayed by B mode of operation was used for precise time measurements. This mode permitted the start of A sweep to be delayed for a selected time after the signal event with the greatest amplitude (in the present case it was the ~~original~~ pulse). In this mode of operation any event within a series of events could be displayed in a magnified form with a total horizontal magnification of 100X. Further, the calibrated delay time multiplier could be used to bring each event on a fixed marker on the screen and time between successive events could be directly read on the delay time multiplier dial. The smallest delay time measurable with the delay time multiplier was 1% of the delay time used, in the present case 2  $\mu$ secs, i.e., about 0.02  $\mu$ sec. Any shorter delay time could be measured by proper calibration of the delay time multiplier and interpolation between two small divisions. Time measurements with certainty could be made down to 0.01  $\mu$ sec. Before use, the two time bases were checked and calibrated against a Type 180A Tektronix time



mark generator. To increase further the accuracy of measurement, instead of measuring delay time between two echoes, wherever it was possible, a number of echoes could be chosen. A photograph of the whole equipment is shown in Fig. 5 and a typical longitudinal wave echo train for Aluminium at room temperature is shown in Fig. 6.

### 2.3 Operation and Performance of the Pulse-Echo Equipment

The performance of the equipment was tested with a polycrystalline copper specimen made from a 99.99 pct. pure stock supplied by M/s. Semi Elements Inc., New York, U.S.A. Copper was chosen for this purpose because of the fact that good agreement was found to exist between velocity data reported by various workers<sup>54-56</sup>. Copper from the stock was melted in a recrystallised alumina crucible. The cast metal was lightly cold forged and subsequently annealed at 700°C for 2 days. The annealed sample was then machined to produce a cylindrical specimen of 10 mm dia and 8 mm length. The machined specimen was annealed again at 500°C for 4 hours. The specimen was then metallographically polished. The two parallel surfaces of the pure copper specimen were carefully cleaned with acetone and on one of them a thin layer of bonding agent (such as Dow Corning 200 Silicone fluid or Nonaq stop-cock grease) was applied. The transducer was then carefully pressed on to

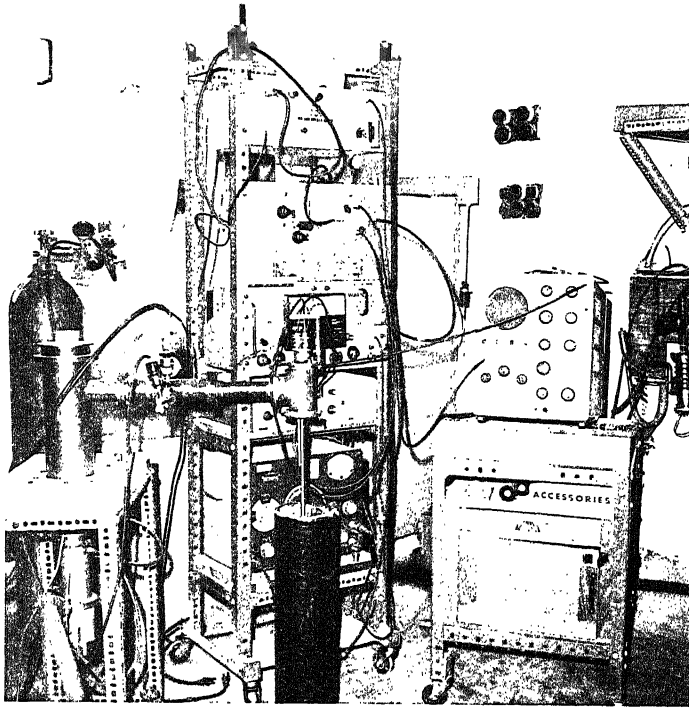


**Fig. 5** A photograph of the pulse - echo equipment

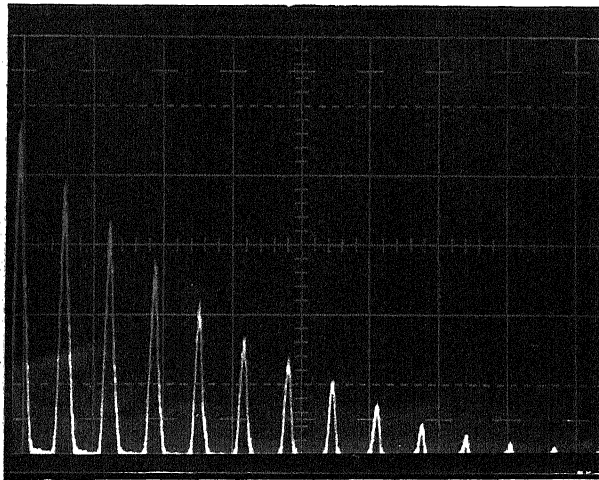


**Fig. 6** Longitudinal wave echo train in Aluminum at room temperature

the greased specimen surface and the excess fluid was wiped out. The specimen was then placed between the copper contact points of the specimen holder. The can was soldered in its place and the specimen chamber was evacuated with the help of the vacuum system. The specimen holding assembly was slowly lowered into liquid nitrogen when a vacuum better than  $5 \times 10^{-6}$  mm of Hg was obtained. No test with liquid He was performed. A small amount of He gas was introduced into the specimen chamber and within 15 minutes the specimen temperature went down close to  $77^{\circ}\text{K}$  and within 30 minutes a stable  $77^{\circ}\text{K}$  temperature could be obtained.

For the present work measurements were carried out between  $77^{\circ}\text{K}$  and room temperature and the above method of operation was not used. The can was detached from the specimen holder and the velocity of longitudinal ultrasonic waves was measured at room temperature. Then the specimen holder was inserted into a 30" long and 4" dia dewar flask covered with a styrofoam block. The bottom 4" of the dewar was filled with liquid nitrogen. The specimen was dipped in the liquid nitrogen bath and the velocity was measured. It was then lifted out of the bath and kept very close to the surface of liquid  $\text{N}_2$ . In about 15 to 20 minutes time the specimen temperature stabilized to a higher value and the temperature was found to be within

$\pm 1^{\circ}\text{K}$  for about 10 minutes. This time was sufficient to make the velocity measurements. In this way, by adjusting the position of the specimen above the liquid nitrogen level any desired temperature between  $77^{\circ}\text{K}$  and about  $300^{\circ}\text{K}$  could be easily obtained. The details of the procedure for operating the equipment and the switch positions for the electronic equipments are given in Appendix A.

Due to very high attenuation of ultrasonic waves in copper, only two observable echoes were available for measurement. The echo time was measured at  $77^{\circ}\text{K}$  and  $300^{\circ}\text{K}$ . The observed data and the averaged longitudinal wave velocity of copper calculated from the single crystal data<sup>55</sup> is given in Table 5.

The success of the measurement depends on good bonding of the specimen and the transducer. Nonaq stop cock grease has been recommended for bonding at low temperature<sup>57</sup>. However, in the present investigation the performance of this material between about  $100^{\circ}\text{K}$  and  $250^{\circ}\text{K}$  was not found satisfactory. Performance of DC 200 silicone fluid was better in this temperature range than around room temperature. Several measurements at room temperature with DC 200 fluid had to be confirmed with experiments using the Nonaq grease.

Table 5 : Longitudinal wave velocity in copper

Temp °K	Delay time <sup>+</sup> μsec	Velocity observed μM/sec	Velocity calc. M/sec <sup>55</sup>
77	3.19	4881	4828
306	3.28	4762	4726

<sup>+</sup>Specimen Length = 7.815 mm

## CHAPTER 3

### X-RAY DIFFRACTOMETER ATTACHMENT FOR LOW TEMPERATURE

As given in Eqn. 3 , the number of independent mass centres per unit volume is needed to evaluate  $\Theta_D$  and this can be easily obtained if the lattice parameter and crystal structure of the material is known. To determine precise lattice parameter as a function of temperature a diffractometer was considered reasonably accurate and convenient. Thus for GE - XRD/V diffractometer a low temperature attachment to work between 77°K and room temperature was designed.

The low temperature attachment for the X-ray diffractometer should essentially provide the following facilities, a) easy specimen alignment with respect to the X-ray beam, b) bringing down the temperature of the specimen close to 77°K, c) providing minimum heat leakage to the specimen, d) heating up the specimen to any desired temperature & e) maintaining the specimen temperature at any desired level for proper recording of the diffraction pattern. Keeping these points in mind the low temperature attachment shown in Fig. 8 was designed to work between 77°K and room temperature and the block diagram for the low temperature attachment is shown in Fig. 7.

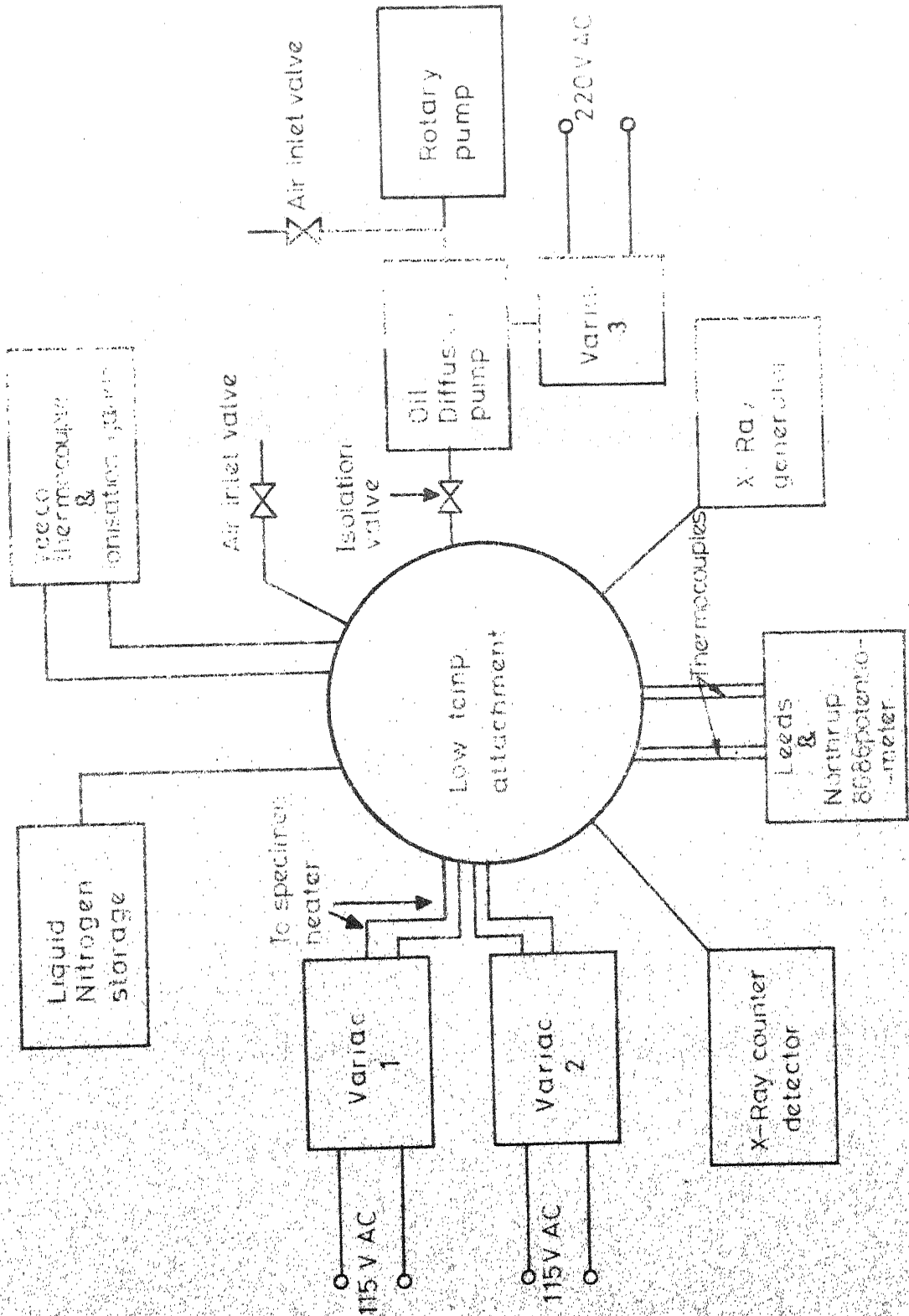
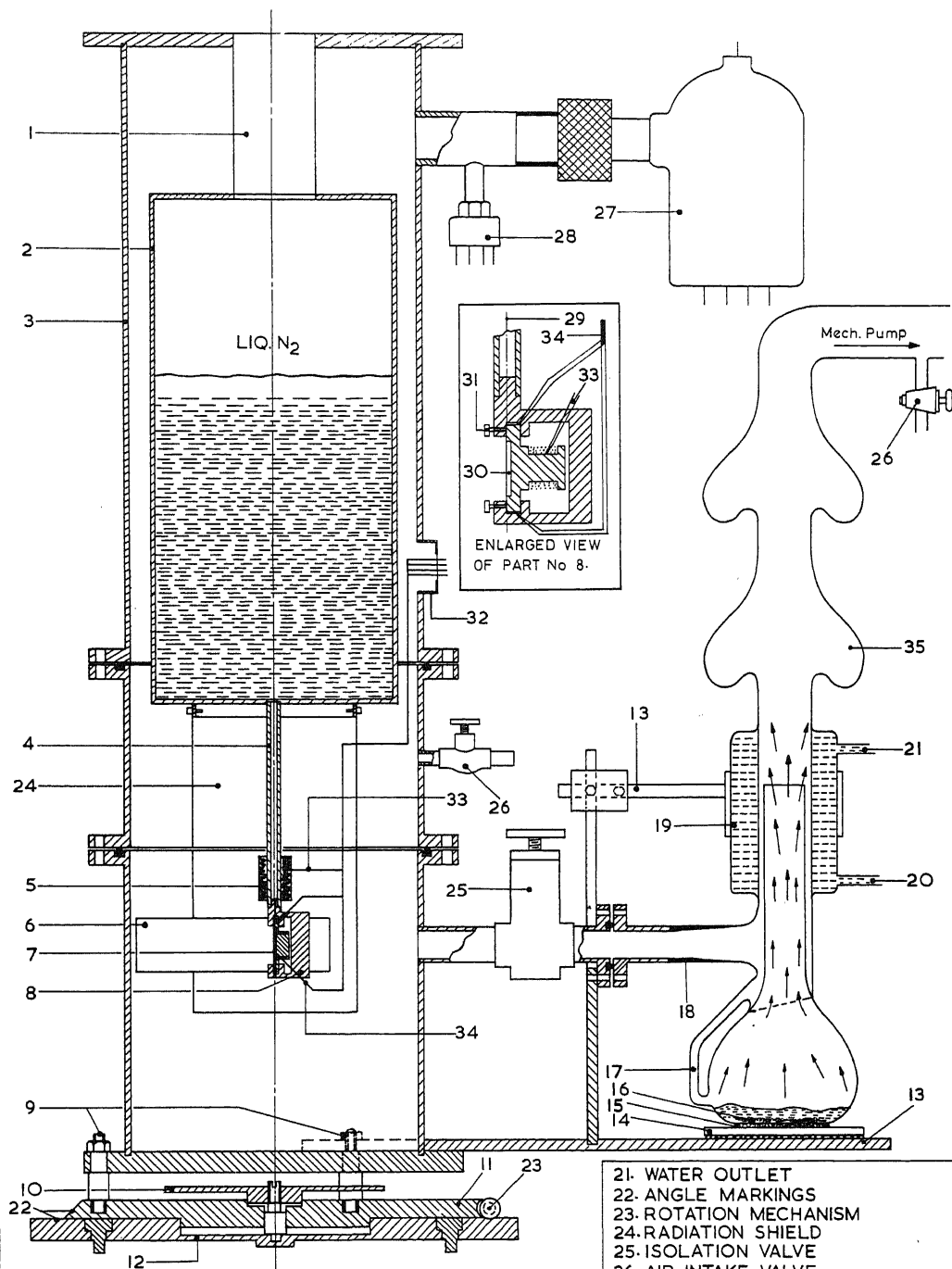


Fig. 7 Block diagram of the low temperature attachment.



- 1-THINWALL S.S.TUBE.
- 2-LIQ. N<sub>2</sub>TANK.
- 3-OUTER SHELL
- 4-SPECIMEN HOLDER TUBE
- 5-HEATER
- 6-0.01" Be. WINDOW
- 7-SPECIMEN
- 8-SPECIMEN HOLDER
- 9-SPACERS
- 10-LOCK NUT
- 11-ROTATING BASE PLATE
- 12-FIXED BASE PLATE
- 13-DIFFUSION PUMP SUPPORT
- 14-DIFFUSION PUMP HEATER
- 15-ASBESTOS POWDER
- 16-OIL BATH
- 17-OIL FEED BACK
- 18-GLASS TO METAL JOINT
- 19-WATER COOLER
- 20-WATER INLET
- 21-WATER OUTLET
- 22-ANGLE MARKINGS
- 23-ROTATION MECHANISM
- 24-RADIATION SHIELD
- 25-ISOLATION VALVE
- 26-AIR INTAKE VALVE
- 27-IONISATION GAUGE
- 28-THERMOCOUPLE GAUGE
- 29-DIFFRACTOMETER ROTATION AXIS
- 30-SPECIMEN PLATE
- 31-TIGHTENING SCREWS
- 32-MULTITERMINAL HEADER
- 33-HEATER CONNECTION
- 34-THERMOCOUPLES
- 35-GLASS DIFFUSION PUMP



The low temperature attachment for diffractometer essentially had two parts, a) the liquid  $N_2$  tank with the specimen holder, and (b) the base of the attachment consisting of X-ray window, specimen alignment features and vacuum attachments. The following sections give details of the equipment and its test performance.

### 3.1 The Liquid Nitrogen Tank

The liquid nitrogen tank (2) had a capacity of about 2 litres and was made of a thin walled copper tube closed at the bottom by a thin copper flange. The tank was coaxially suspended from the top covering plate of the outer shell (3) with the help of a thin wall (1.12" dia, 0.01" wall thickness) stainless steel tube (1). To the bottom of the tank a 0.375" dia copper tube (4) was silver brazed. At the other end of this tube the specimen holder (8) was attached. The holder was machined out of a cylindrical copper block such that the specimen surface (7) was always coplanar with the diffractometer rotation axis (29). The specimen plate (30), made of copper, was with a 1" x 1" x 0.03" groove to hold the specimen powder. The specimen plate snugly fitted into the holder and two tightening screws (31) were provided to ensure good thermal contact between the specimen plate and the plate holder. To reduce the thermal leak to the specimen by radiation

a detachable radiation shield (24) was attached to the bottom of the tank. Two heaters (5,33) were provided on the copper tube and the specimen plate to heat up the specimen and to maintain the desired elevated temperature above  $77^{\circ}\text{K}$ . Two copper - constantan thermocouples (34), attached to the specimen plate, measured the temperature at the top and bottom ends of the plate. The connections for the thermocouples and heaters were led out of the outer shell through a multiterminal Kovar plug (32) attached to the body of the outer shell.

### 3.2 The base of the Attachment

The base, with the vacuum system, was designed to fit on the central platform of the spectrogoniometer of the GE - XRD - V or VI X-ray diffractometer. On the outer shell (3) a 1" wide opening (6), covering an angular range of  $200^{\circ}$ , was cut and a 0.01" thick Be - foil was attached to it with the help of Hysol epoxy adhesive resin. The Be foil served as the X-ray window. The shell was closed at the bottom by a brass plate, which was supported by three spacer studs (9). The support for the diffusion pumps (3) was also attached to the brass plate. A light weight diffusion pump (13), made of glass and with an O-ring flange at the end of the Kovar high vacuum end (18),

was connected to the outer shell (3) through an isolation valve (35). About 20 cc diffusion pump oil could be used in the diffusion pump. The oil was heated from outside with the help of a heater (14) also supported by the same diffusion pump support. A 140 lit/minute capacity mechanical pump, mounted on a movable trolley, was connected to the diffusion pump through a 3' long 0.875" dia rubber hose to enable free rotation of the diffusion pump with the rotation of the spectrogoniometer. The photograph of the equipment is shown in Fig. 9. The flexibility of the rotation of the diffusion pump was, however, limited to about  $60^\circ$  in the 2 $\theta$  scale. Depending on the angular region to be studied, the position of the mechanical pump had to be changed.

The spacer studs supporting the base were fixed on a brass plate (11) which could rotate with respect to the plate (12) attached with the diffractometer platform by holding screws. A worm and gear arrangement (23) was provided for rotation of the plate (11). A vernier scale (22) with a least count of  $0.05^\circ$  was engraved on the bottom plate and a main scale was engraved on the rotating plate. Further adjustment for alignment of the specimen holder was made by making the specimen tilt back and forth by adjusting the spacer studs. Once the proper position of the specimen was obtained on the diffractometer through the

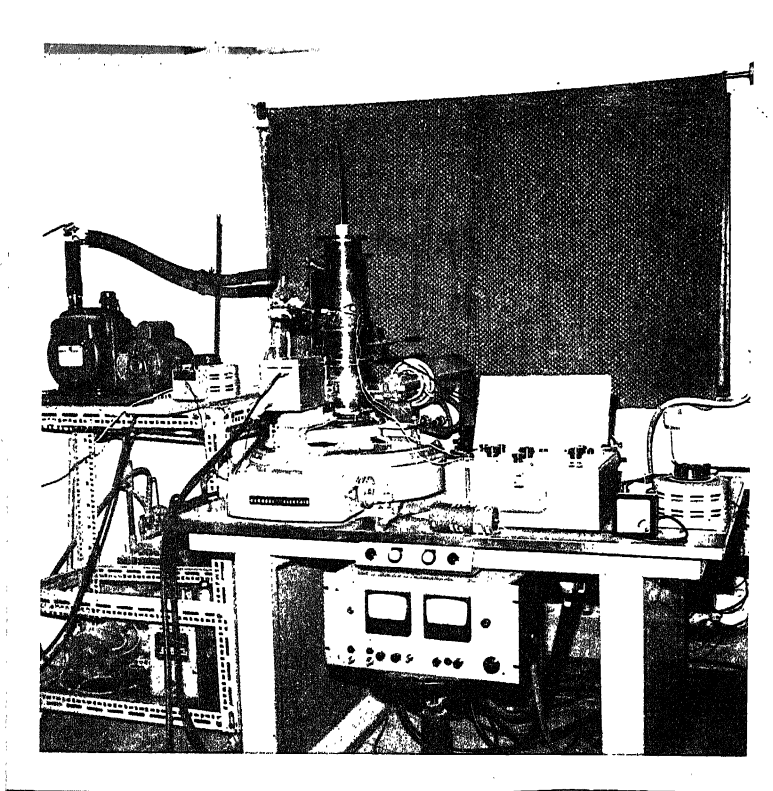


**Fig. 9** A photograph of the low temperature attachment

tilting and rotating devices the lock nut (10) could be tightened to prevent accidental rotation of the low temperature attachment.

An intermediate cylindrical part, to which an air inlet valve (26) was attached, was used to facilitate easy servicing of the main two parts. Necessary guide pins and matching holes were provided on the adjacent flanges of the three parts for easy alignment of the parts and to ensure that no major change in the specimen position occurred once the position of the base plate was fixed.

### 3.3 Operation and Performance of the Low Temperature Attachment

After cleaning the specimen plate with acetone the specimen powder was pressed into the groove with a clean glass slide and the pressed powder was levelled by scraping with the edge of the glass slide till the powder specimen surface was flush with the rim of the specimen plate. The specimen plate was fixed in the holder with the help of the fixing screws, the heater connections were made and the two thermocouples were soft soldered with the specimen plate. After checking the alignment of the specimen, the diffraction line positions at room temperature were determined. The isolation valve was closed and the initial evacuation was started with the mechanical pump. The isolation valve

was opened very slowly to avoid sudden evacuation of the low temperature attachment. This was necessary to prevent the powder from falling off the specimen plate. When with the help of the diffusion pump the inside pressure went below  $10^{-4}$  mm Hg liquid  $N_2$  was poured into the nitrogen tank of the low temperature attachment. Almost immediately the pressure inside began to fall and in about 20 mins of it came down to about  $2 \times 10^{-5}$  mm of Hg. In about 30 minutes the specimen temperature came down to a stable  $89^\circ K$ . The specimen temperature measured with the two thermocouples differed by only  $1^\circ K$ .

For taking the specimen to any intermediate temperature, the input voltage to the two heaters was increased and the system was allowed to come to equilibrium. After a lapse of 20 to 30 minutes, the usual time taken by the specimen to come to a stable temperature, the temperature was measured and if it remained constant (to within  $\pm 1^\circ K$ ) for more than 10 minutes diffraction peak position was determined. Due to the use of 40 gauge manganin wire, which was suitable for use at low temperatures, the heaters could not be used above  $250^\circ K$ . In order to avoid damage to the heaters all measurements were carried out between  $89^\circ K$  and  $230^\circ K$ .

Since a glass diffusion pump was used, a continuous, scanning method for record of the diffraction peak was not possible. This however was not a real limitation for the present purpose because a step scan method was used. The step scan method is superior to the continuous scanning method because no peak shift due to rate of scanning occurs. For the estimation of lattice parameter the diffraction peaks in the  $2\theta$  angular range of  $100^\circ$  to  $145^\circ$  were recorded using a manual step scan method with a 40 sec counting time. A typical diffraction peak for Al at  $89^\circ\text{K}$  and  $306^\circ\text{K}$  is shown in Fig. 10.

To test the performance of the low temperature attachment at room temperature pure Al powder (99.9 pct. pure, supplied by semi-elements Inc., New York) was used. Four reflections, (111), (311), (331) and (420), were recorded using  $\text{NiK}_\alpha$  radiation at 50 KV and 9 mA. For comparison, the same Al powder specimen was used for taking a diffraction pattern using the room temperature holder of the GE diffractometer. The lattice parameter data calculated from the four reflections for both the low temperature attachment and the room temperature holder are shown in Table 6 and Fig. 11. It is clear from the figure that the systematic errors for small angles are comparatively large for the low temperature attachment but is of the same order as the room temperature holder at the high angle

**Fig. 10 The (420) reflection for Al at two temperatures showing  $\alpha_1$  and  $\alpha_2$  peaks**



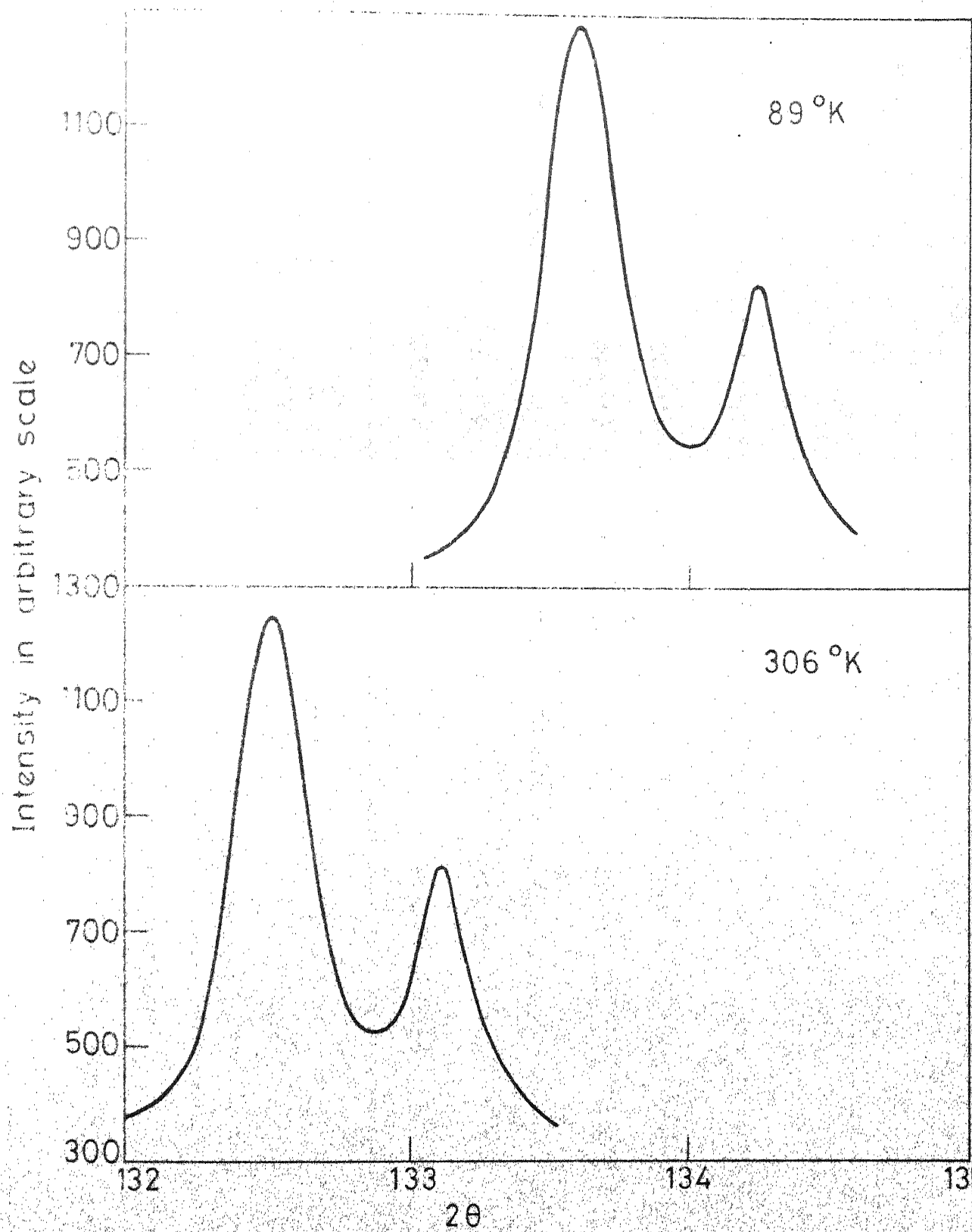


Fig. 10

Table 6 : The peak positions and lattice parameters of Aluminium as obtained at (306°K) by using the spectrogoniometer specimen holder and the low temperature attachment.

h k l	<u>Spectrogoniometer holder</u>		<u>Low Temperature attachment</u>		L.P. reported [Ref. 75]
	2 $\theta$ °	L.P. °(Å)	2 $\theta$ °	L.P. °(Å)	
1 1 1	41.52	4.0504	41.525	4.0499	4.04968 (at 298°K)
3 1 1	95.50	4.0500	95.51	4.0498	
3 3 1	126.30	4.0498	126.30	4.0498	
4 2 0	132.52	4.0498	132.52	4.0498	

**Fig. 11** Lattice parameter of Al at room temperature obtained with two specimen holder

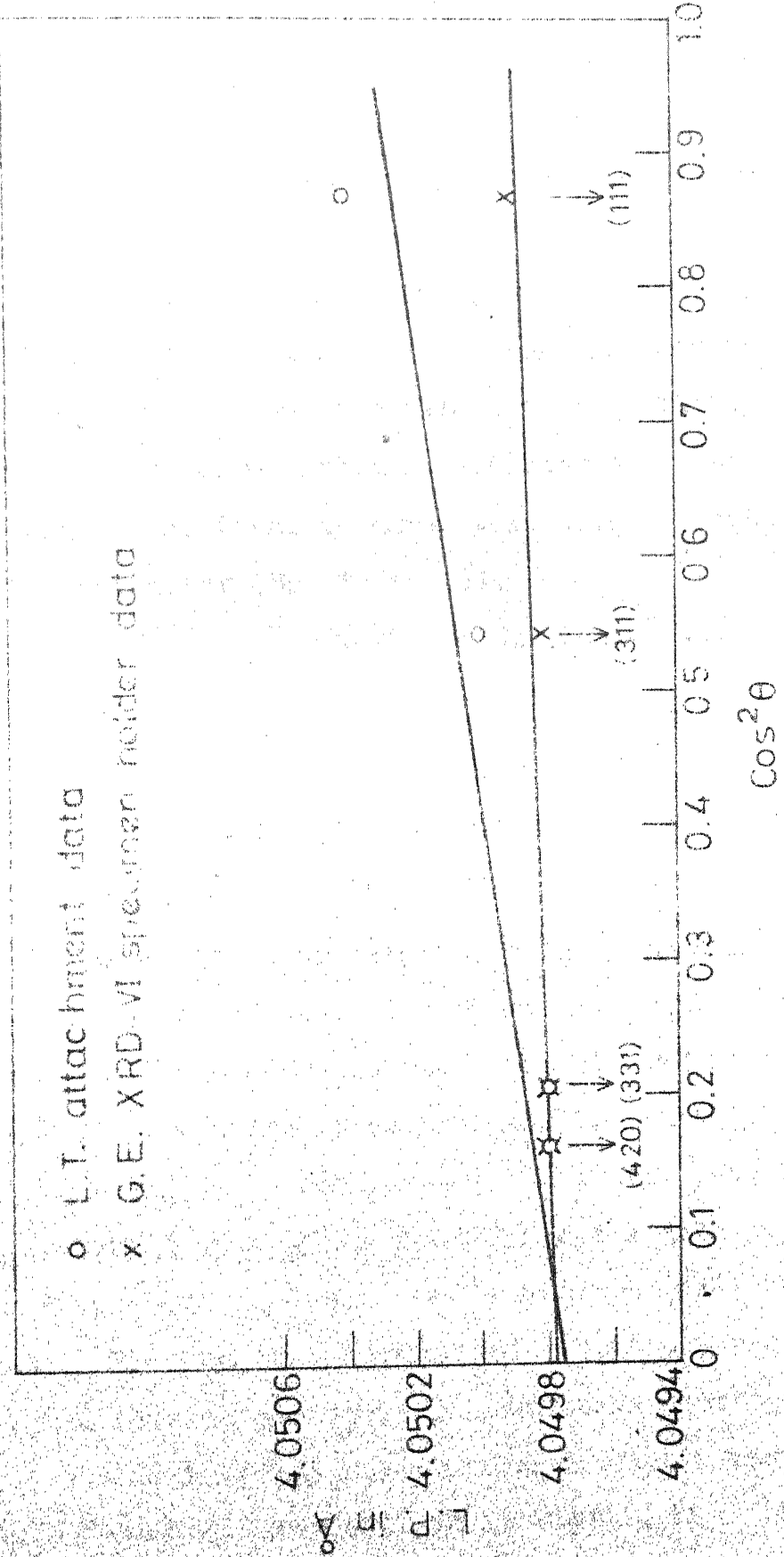


Fig. 11

Table 7 : Observed Lattice parameter of Aluminium  
at different temperatures

---

$a_0^{\circ}(\text{\AA})$	Temp. $^{\circ}\text{K}$
4.0330	89
4.0335	102
4.0349	129
4.0358	142
4.0390	185
4.0498	306

---

Table 7 : Observed Lattice parameter of Aluminium  
at different temperatures

---

$a_0$ (Å)	Temp. °K
-----------	----------

---

4.0330	89
--------	----

4.0335	102
--------	-----

4.0349	129
--------	-----

4.0358	142
--------	-----

4.0390	185
--------	-----

4.0498	306
--------	-----

---

**Fig. 12** Measured lattice parameter of Al at low temperatures and calculated lattice parameter on the basis of room temperature lattice parameter and thermal contraction data van Arp et al [Ref.58] published by NBS

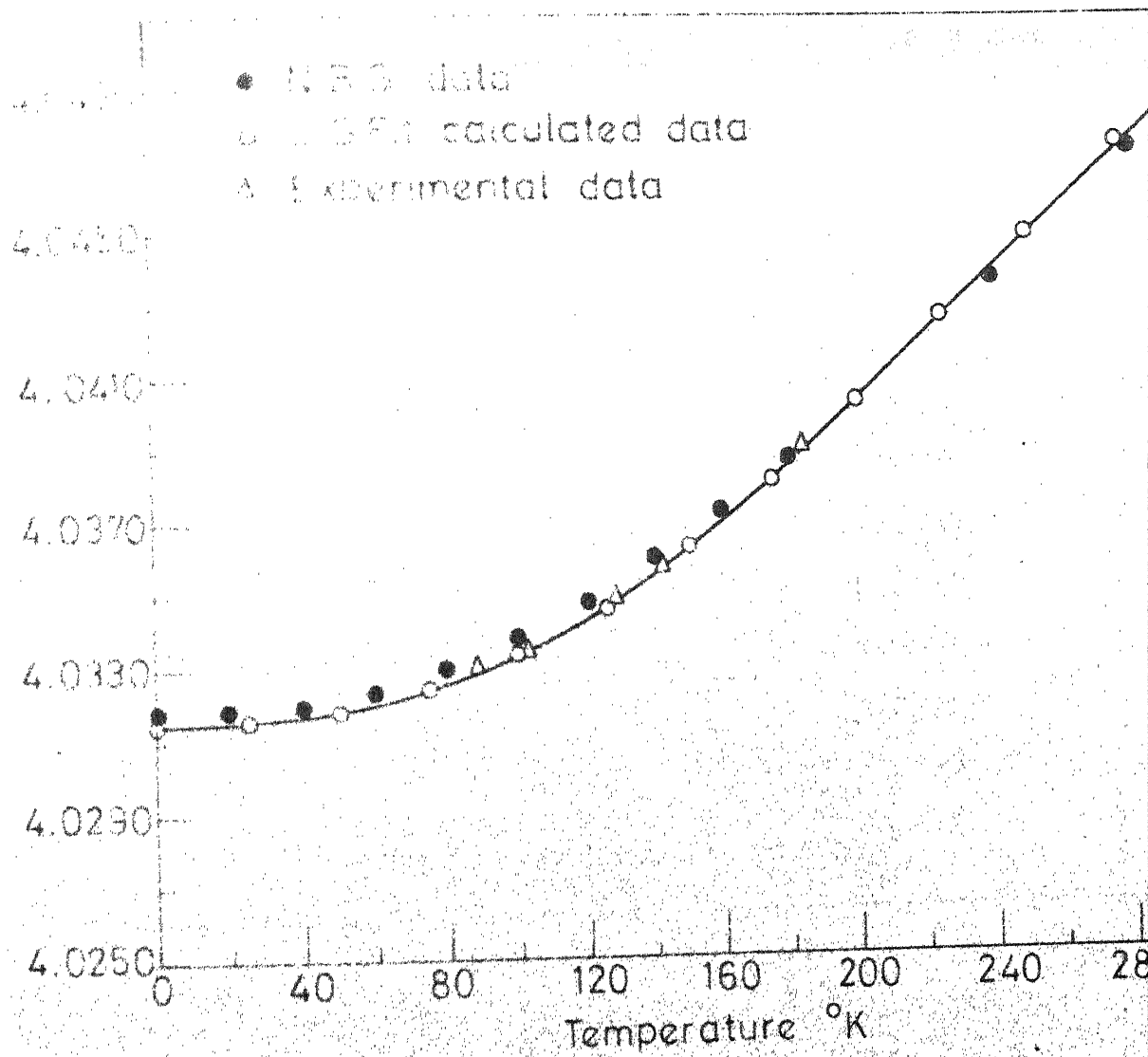


Fig. 12



Table 8 : Low temperature lattice parameter of Al  
calculated on the basis of van Arp's thermal  
contraction data published by NBS<sup>58</sup>.

Temp <sup>°</sup> K	Lattice parameter $\overset{\circ}{\text{\AA}}$
20	4.0319
40	4.0320
60	4.0324
80	4.0330
100	4.0338
120	4.0349
140	4.0360
160	4.0373
180	4.0388
200	4.0403
240	4.0430
280	4.0472

## CHAPTER 4

### EXPERIMENTAL PROCEDURE

#### 4.1 Preparation of Specimens

In this investigation pure Al and Al-Zn alloys were used. The alloys were made from 99.9% pure Aluminium and 99.9% pure Zinc supplied by M/s. Semi Elements Inc., U.S.A. The Al-rich side of the Al-Zn phase diagram<sup>59</sup> is shown in Fig. 13. Aluminium has about 4 at.pct. solubility for Zinc at room temperature. Higher Zn containing alloys in super-saturated condition give rise to clusters at room temperature very quickly<sup>60</sup>. In the lower Zn concentration (<15 at.pct. Zn) regions, however, the alloys can be kept in the quenched super-saturated state without any cluster formation for at least 10 mins. On the basis of the above limitations the alloys were chosen to contain 1, 2, 3, 4, 10 and 15 at. pct. Zn.

The pure aluminium specimen and alloy specimens with land 2 at. pct. Zn were melted in a high frequency induction melting unit under protective Argon gas atmosphere. The rest of the four higher Zn containing alloys were melted in an open pit furnace using borax flux and chill cast in a 12.5 mm dia split mould made of mild steel. As found in trial meltings, the Zinc loss due to vaporization was about 1 pct and was taken care of in the charge

. calculation. The alloys were analysed for Zinc using wet assay method and Al content was found by difference. Table 9 gives the intended and the analysed compositions of the alloys. All specimens after casting weighed about 50 to 60 gms.

The cast specimens were then cut to about 4 cm long pieces and sealed in pyrex glass tubes under Argon gas at 1000 microns pressure. The specimens were then annealed at  $300^{\circ}\text{C}$ . for 72 hrs to homogenise the cast structure and subsequently water quenched. The homogenised specimens were then cut to two smaller pieces of length about 2.5 cms and 1.5 cms.

The longer part was used for the preparation of the specimens for ultrasonic studies. It was heated to  $300^{\circ}\text{C}$  and hot forged slightly from all directions to ensure random grain orientation. During forging a close watch was kept on the formation of cracks and in cases of doubt the specimens were rejected. The forged specimens were then machined on a precision lathe to produce cylindrical specimens of about 10 mm dia and 16 mm length. The final shaping was done on a milling machine to have two parallel and plane surfaces. The length of the specimen at this stage was about 10 mm. Final preparation of the two flat surface were done by polishing on wet polishing wheels with

Table 9 : Tentative and analysed composition of the alloys

Tentative Composition in atomic percent		Analysed Composition in atomic percent	
Al	Zn	Zn	Al
99	1	0.7	99.3
98	2	2.4	97.6
97	3	3.3	96.7
96	4	4.5	95.5
90	10	8.6	91.4
85	15	13.9	86.1

0.5 micron alumina powder. Very low pressure was applied during polishing and a low speed of the wheel was found to give satisfactory polishing. To remove the strains produced during machining the specimens were sealed under vacuum in pyrex tubes and annealed at  $250^{\circ}\text{C}$  for 4 hrs. and water quenched. The length of the quenched specimens was measured by a Sheffield Accutron Electronic Comparator. The surface unevenness was found to be of the order of  $\pm 0.002$  mms. About 30 measurements were made for each specimen and the average values were used for velocity calculations. For the  $\text{Al}_{90}\text{Zn}_{10}$  and  $\text{Al}_{85}\text{Zn}_{15}$  alloys this procedure was not followed. The details of the alternative procedure are given in Sec. 4.2.

The smaller portion of the homogenised specimens were utilized for X-ray studies. An acid cutting unit for single crystals was modified to work as a continuous filing machine. The acid string was replaced by a fine hard file and the to and fro movement of the string was used for moving the file. The alloy pieces were vacuum sealed and annealed at  $250^{\circ}\text{C}$  for 48 hrs and water quenched. The specimens were fixed on the single crystal holder of the acid cutting unit. In this method sufficient powder for X-ray studies could be collected in about 50 hrs. The powder was then screened with a 300 mesh seive. The finer powder was again vacuum

sealed, annealed at  $250^{\circ}\text{C}$  for 20 minutes and water quenched. The powder was then placed in the specimen holder of the low temperature attachment for X-ray diffraction studies. This procedure was not followed for the  $\text{Al}_{90}\text{Zn}_{10}$  and  $\text{Al}_{85}\text{Zn}_{15}$  alloys. the details of the alternative procedure are given in Sec. 4.3.

#### 4.2 Procedure for Operation of the Ultrasonic Equipment with High Zn Alloys

According to the Al-Zn constitution diagram (Fig. 13) and the work of Panseri et al<sup>60</sup> it is known that upto 4 at.pct. Zn in Al the single phase characteristics of the alloy can be retained whereas for the higher Zn alloys (10 and 15 at.pct.Zn) the single phase without formation of any clusters can be retained if the alloy is quenched to room temperature and within 10 minutes cooled down  $50^{\circ}\text{K}$  below room temperature. Because of this a different procedure had to be adopted for the two high Zn alloys.

Immediately after quenching from  $300^{\circ}\text{C}$ , the length of the samples were measured by a micrometer screw gauge. The sample was cleaned and DC-200 silicone fluid was applied on one plane surface. The transducer was fixed and the specimen was fitted in the specimen holder. The specimen holder was immediately immersed in liquid Nitrogen. This way, the specimen was kept at room temperature for less

than 3 minutes. Then the adjustments were done for the electronic systems (Appendix A) and data were taken upto about  $220^{\circ}\text{K}$ . Beyond this temperature no further data was taken due to the fact that close to room temperature the clustering, zone formation and precipitation reactions are expected to start.

#### 4.3 Procedure for Operation of the X-Ray Attachment for High Zn Alloys

Due to the same reasons as mentioned above a special procedure for the X-ray study of the two high Zn alloys was used. Immediately after quenching, the powder was filled in the specimen plate without any binder. The plate was fixed in the specimen holder and the top part of the attachment was connected with the bottom part. The mechanical pump was started with the isolation valve closed and once the initial pump noise subsided, the isolation valve was slowly opened. Throughout the process of opening of the isolation valve the X-ray equipment was kept running and watch was kept on the peak intensity after manually fixing the spectrogoniometer on the  $2\theta$  corresponding to the (420) peak. When the vacuum reached about .50 microns in 2 to 3 minutes and it was made sure that the specimen surface was not damaged (i.e. the peak intensity did not fall) about 0.5 litres of liquid nitrogen was poured in the

tank giving rise to heavy frosting of the whole equipment. This resulted in reducing the temperature of the specimen to about  $200^{\circ}\text{K}$ . The oil diffusion pump was then operated and in about 30 minutes time, the vacuum improved to about  $2 \times 10^{-5}$  mm of Hg and the frost melted out. The attachment was wiped dry and more liquid Nitrogen was poured in. This procedure, though quite cumbersome, helped in reducing the specimen temperature below  $200^{\circ}\text{K}$  within 6 to 7 minutes of quenching. The X-ray diffraction data for the 10 and 15 at.pct. Zn alloys were not collected in the temperature range of  $220^{\circ}\text{K}$  to  $300^{\circ}\text{K}$ .

#### 4.4 Calibration of Thermocouples

Four copper - constantan thermocouples, two each for the two equipments were calibrated against the boiling point of liquid nitrogen, freezing points of ethyl alcohol, acetone and water. The e.m.f. of the thermocouples were measured by a Leeds and Northrup 8686 potentiometer with the hot junction in ice and water mixture. Table 10 shows the results of the calibration. A comparison of the calibration data of copper - constantan thermocouple was made with the e.m.f. - temperature chart published by M/s. Omega Engineering Inc., Stanford, U.S.A. Since no major difference in the corresponding e.m.f. values were observed, the chart was used to convert the thermocouple e.m.f. values to temperature.



Table 1      The observed e.m.f. values for the thermocouples at the calibration points.

Bath	Fixed Temp. (°K)	e.m.f. in mv				
		T.C. No.1	T.C. No.2	T.C. No.3	T.C. No.4	Chart <sup>+</sup>
Liq. Nitro- gen	77	-5.47	-5.46	-5.47	-5.47	-5.46
Ethyl Alco- hol	156	-3.82	-3.82	-3.83	-3.82	-3.82
Acetone	178	-3.21	-3.21	-3.21	-3.21	-3.21
Water	273	0.00	0.00	0.00	0.00	0.00

<sup>+</sup> Chart published by M/s. Omega Engineering Inc.  
Stamford, U.S.A.

## CHAPTER 5

### RESULTS

Velocity of 10 MHz longitudinal and shear waves were determined as a function of temperature using the pulse - echo equipment. Since large number of echoes for longitudinal waves could be obtained (Fig. 6), the pulse-echo delay time could be measured using several echoes. In practice, however, the delay time multiplier of time base B (545B Tektronix Oscilloscope) gave a maximum delay of 20  $\mu$ secs which could accomodate only six successive echoes for measurement. In case of the shear waves, only two successive echoes could be obtained and accordingly, the delay time was measured with only two echoes. Thus, the velocity of longitudinal waves could be determined with higher accuracy. Tables 11,13,15,17,19,21 and 23 and Fig. 14 shows the delay time and velocity of longitudinal waves in the specimens between 77°K and 306°K and Tables 12,14, 16,18,20,22 and 24 and Fig. 15 shows the delay time and velocity of shear waves in the specimens between 77°K and 250°K. The lattice parameters of Al and Al-Zn alloys were determined using the low temperature attachment with the help of the (420) reflection and the variation of lattice parameters with temperature for the specimens are shown in

Tables 7 and 25 to 30 and Fig. 16.

The measured data were used to derive the values of thermal expansion coefficient,  $\Theta_D$ , bulk modulus, shear modulus and Young's modulus between  $0^\circ\text{K}$  and  $300^\circ\text{K}$ . The measured values of  $v_l$ ,  $v_s$  and  $\rho_0$  were fit by the least square method with a fourth order polynomial in temperature of the form  $F_T = F_0 + AT + BT^2 + CT^3 + DT^4$  such that the slope of the curve against  $T$  goes to zero as  $T \rightarrow 0^\circ\text{K}$ . The least square fit of data were obtained with an IBM 7044 electronic computer using double precision. It has been theoretically justified<sup>61</sup> that the rate of change of elastic constants and hence of the velocities and  $\Theta_D$ , is zero at  $T = 0^\circ\text{K}$ . Using the values of  $v_l$ ,  $v_s$  and lattice parameter corresponding to the polynomial  $\Theta_D$  (from Eqn. 15) bulk modulus (from Eqn. 21), shear modulus (from Eqn. 22), thermal expansion coefficient and Young's modulus ( $Y$ ) (from the relation  $\frac{3}{G} + \frac{1}{K} = \frac{2}{Y}$ ) were calculated at every  $25^\circ\text{K}$  from  $0^\circ$  to  $300^\circ\text{K}$ . Tables 32 to 38 give the calculated parameters and the standard deviations for the L.S. fit. Fig. 17 shows the variation of  $\Theta_D$  with temperature and Fig. 18 shows the variation of  $0^\circ\text{K}$  values of  $\Theta_D$ , bulk modulus and shear modulus with composition.

In both the velocity and lattice parameter measurements, temperature was kept constant within  $\pm 1^\circ\text{K}$ . The error in specimen length variation or lattice parameter variation during measurements, due to this variation in temperature is small and has been neglected. The other errors may be grouped as (1) Instrumental Errors (2) Random Errors. The instrumental errors in the evaluation of velocities and  $\Theta_D$  are shown in Table 31. It is clear that the errors are quite small and the final data for  $\Theta_D$  is correct to about 1 pct. In the calculation of errors, no allowance was made for transit time errors which are quite small and varies between 0.02 to 0.1  $\mu\text{sec}$ .<sup>63-64</sup> In the present work, the transit time due to the passage of the pulse-echoes through the bond and the transducer did not affect the results, since the delay time measurements were made with successive echoes and not with respect to the original pulse.

Table 11 : Measured Longitudinal wave velocity in  
Aluminium  
Specimen size = 1.033 cms

Delay Time $\mu$ sec.	Velocity M/sec	Temp <sup>o</sup> K
3.183	6465	77
3.187	6458	90
3.187	6458	112
3.190	6451	123
3.197	6444	149
3.203	6431	180
3.220	6404	207
3.227	6390	230
3.245	6364	267
3.263	6331	291
3.273	6312	311

Table 12 : Measured shear wave velocity in Aluminium  
Specimen size = 1.033 cms

Delay Time $\mu$ sec.	Velocity M/sec.	Temp <sup>o</sup> K
6.44	3196	77
6.44	3196	91
6.46	3186	110
6.46	3186	127
6.48	3179	159
6.52	3160	186
6.56	3146	221
6.62	3119	253

Table 15 : Measured longitudinal wave velocity in  
aluminium 1 percent Zn alloy.  
Specimen size = 1.035 cm

Delay Time	Velocity (M/sec)	Temp. <sup>o</sup> K
3.197	6450	77
3.198	6447	91
3.200	6444	108
3.203	6437	128
3.210	6430	155
3.217	6417	174
3.227	6403	198
3.233	6390	217
3.253	6357	257
3.275	6324	289
3.283	6304	313

Table 16 : Measured shear wave velocity in Aluminium  
1 percent Zn alloy. Specimen size = 1.035 cm

Delay Time μ sec.	Velocity (M/sec.)	Temp. <sup>o</sup> K
6.48	3182	77
6.49	3177	110
6.50	3172	127
6.54	3156	166
6.58	3140	195
6.65	3114	233

Table 15: Measured Longitudinal wave velocity in  
aluminium 2 percent Zn alloy.

Specimen size = 1.021 cm

Delay Time $\mu$ sec.	Velocity (M/sec)	Temp <sup>o</sup> K
3.190	6376	77
3.190	6376	89
3.193	6370	102
3.197	6365	114
3.205	6349	160
3.220	6329	186
3.227	6316	208
3.237	6297	244
3.260	6258	274
3.280	6226	313

Table 16 : Measured shear wave velocity in aluminium  
2 percent Zn alloy.

Specimen size = 1.021 cms.

Delay Time $\mu$ sec.	Velocity (M./sec.)	Temp <sup>o</sup> K
6.52	3120	77
6.54	3110	109
6.54	3110	133
6.56	3104	156
6.61	3079	194
6.66	3060	229
6.70	3042	246

Table 17 : Measured longitudinal wave velocity in Aluminium 3 percent Zn alloy.

Specimen size = 1.019 cms

Delay Time $\mu$ sec	Velocity M/sec.	Temp <sup>o</sup> K
3.207	6331	77
3.210	6326	113
3.213	6317	130
3.218	6311	140
3.220	6304	156
3.223	6293	177
3.240	6278	206
3.260	6245	247
3.273	6222	273
3.297	6182	315

Table 18 : Measured shear wave velocity in Aluminium 3 percent Zn alloy.

Specimen size = 1.019 cms.

Delay Time $\mu$ sec	Velocity M/sec.	Temp <sup>o</sup> K
6.56	3095	77
6.58	3088	112
6.60	3079	141
6.61	3074	154
6.64	3063	177
6.68	3047	205
6.72	3030	228
6.76	3012	246



Table 12 : Measured longitudinal wave velocity in  
Aluminium 4 percent Zn alloy.  
Specimen size = 1.006 cms.

Delay Time $\mu$ sec.	Velocity M/sec.	Temp <sup>o</sup> K.
3.207	6249	77
3.207	6249	84
3.210	6243	117
3.217	6230	138
3.223	6223	163
3.237	6204	192
3.247	6185	222
3.257	6172	243
3.267	6153	267
3.288	6122	291
3.295	6109	312

Table 20 : Measured shear wave velocity in Aluminium  
4 percent Zn alloy.  
Specimen size = 1.006 cms.

Delay Time $\mu$ sec.	Velocity M/sec.	Temp <sup>o</sup> K.
6.56	3055	77
6.58	3046	110
6.60	3036	148
6.64	3021	175
6.67	3004	199
6.74	2982	234

Table 21 : Measured longitudinal wave velocity in  
Aluminium 10 percent Zn alloy.

Specimen size = 1.007 cms

Delay Time $\mu$ sec.	Velocity M/sec.	Temp <sup>o</sup> K
3.297	6079	77
3.298	6076	85
3.300	6073	96
3.300	6070	110
3.307	6066	129
3.313	6054	146
3.320	6042	170
3.333	6024	189
3.350	5994	216

Table 22 : Measured shear wave velocity in Aluminium  
10 percent Zn alloy.

Specimen size = 1.007 cms.

Delay Time $\mu$ sec.	Velocity M/sec.	Temp <sup>o</sup> K
6.92	2896	77
6.94	2888	108
6.96	2882	130
7.04	2842	170
7.08	2836	206
7.14	2812	226

Table 1 : Measured longitudinal wave velocity in  
Aluminium 15 percent Zn alloy.

Specimen size = 1.006 cms

Delay Time $\mu$ sec.	Velocity M/sec.	Temp <sup>o</sup> K
3.430	5848	77
3.432	5845	96
3.435	5842	108
3.440	5837	131
3.447	5825	146
3.457	5809	172
3.470	5792	194
3.477	5781	207

Table 2 : Measured shear wave velocity in Aluminium  
15 percent Zn alloy.

Specimen size = 1.006 cms.

Delay Time $\mu$ sec.	Velocity M/sec.	Temp <sup>o</sup> K
7.18	2794	77
7.20	2786	106
7.22	2780	131
7.24	2773	162
7.30	2753	197
7.34	2738	224
7.38	2726	246

Table 25 : Measured Lattice parameter of Aluminium  
1 percent Zn alloy.

$a_0^{\circ}(\text{\AA})$	Temp $^{\circ}\text{K}$
4.0326	89
4.0329	98
4.0341	122
4.0356	148
4.0376	174
4.0398	201
4.0495	307

Table 26 : Measured Lattice parameter of Aluminium  
2 percent Zn alloy.

$a_0^{\circ}(\text{\AA})$	Temp $^{\circ}\text{K}$
4.0317	89
4.0321	102
4.0329	118
4.0343	141
4.0359	166
4.0390	201
4.0484	304

Table 7 : Measured Lattice parameter of Aluminium  
3 percent Zn alloy.

$a_0$ (Å)	Temp °K
4.0309	89
4.0318	110
4.0335	139
4.0357	174
4.0386	207
4.0478	305

Table 8 : Measured Lattice parameter of Aluminium  
4 percent Zn alloy.

$a_0$ (Å)	Temp °K
4.0301	89
4.0309	112
4.0319	127
4.0342	162
4.0371	199
4.0472	307

Table 38 . Measured Lattice parameter of Aluminium  
10 percent Zn alloy.

$a_0^{\circ}(\text{\AA})$	Temp $^{\circ}\text{K}$
4.0294	89
4.0298	103
4.0307	125
4.0322	147
4.0337	168
4.0377	215

Table 39 : Measured Lattice parameter of Aluminium  
15 percent Zn alloy.

$a_0^{\circ}(\text{\AA})$	Temp $^{\circ}\text{K}$
4.0267	89
4.0273	105
4.0287	133
4.0305	158
4.0324	185
4.0356	220

Table 31 : Instrumental errors entering in the results

Measured Quantity	Critical Measured Quantity	Accuracy	Maximum pet. error		
			$\theta_D$	$v_l$	$v_s$
2	-	$\pm 0.005^\circ$	0.01	-	-
Delay time (l)	20 $\mu$ sec	$\pm 0.02 \mu$	0.01	0.1	-
" " (s)	6 "	" sec	0.64	-	0.4
Specimen length	1 cms	$\pm 0.001$ cms	0.48	0.1	0.1
Total			1.14	0.2	0.5

Table 22 : Bulk modulus, shear modulus, young's modulus and Debye temperature of Aluminium determined through the least square fit of the measured data.

Temp OK	Lattice Para.o (A)	Velocity (Long.) M/sec.	Velocity (shear) M/sec.	Bulk Mod. k bar	Sphear Mod. k bar	Young's Mod. k bar	OK D calc.	Qual. Th. De. Al <sub>2</sub> O <sub>3</sub> /K
0	4.0315	6468	3204	777	283	758	421	0.0
25	4.0316	6468	3203	776	283	758	421	1.9
50	4.0319	6466	3200	776	282	756	421	4.6
75	4.0325	6464	3197	776	282	756	420	7.7
100	4.0334	6459	3192	775	280	750	420	10.9
125	4.0347	6452	3186	773	279	748	419	14.3
150	4.0363	6442	3178	771	277	743	418	17.4
175	4.0382	6429	3169	767	275	738	416	20.0
200	4.0403	6414	3157	763	273	732	414	22.1
225	4.0426	6395	3142	759	270	725	412	23.2
250	4.0449	6374	3122	755	266	715	409	23.2
275	4.0473	6350	3097	751	261	702	406	23.2
300	4.0494	6324	3065	748	256	690	402	23.2

Std. Dev. I.P. =  $0.2 \times 10^{-5}$

Std. Dev.  $v_1 = 16.5$  M/sec.

Std. Dev.  $v_s = 10.8$  M/sec.



Table 59 : Bulk modulus, shear modulus, Young's modulus, coefficient of thermal expansion and Debye temperature of aluminum-1 percent zinc alloy determined through the least squares fit of the measured data.

Temp °K	Lattice Para. (Å)	Velocity (Long.) M/sec.	Velocity (Shear) M/sec.	Bulk Mod. k bar	Shear Mod. k bar	Young's Mod. k bar	Coef. Th. exp. 10 <sup>-6</sup> /°K	GD OK	Calc.
0	4.0311	6453	3186	786	284	761	0.0	419	419
25	4.0312	6453	3186	787	284	761	1.9	419	419
50	4.0315	6453	3185	786	284	761	4.5	418	418
75	4.0321	6450	3183	786	283	758	7.4	418	418
100	4.0330	6446	3179	785	282	756	10.6	418	418
125	4.0342	6439	3172	783	281	754	13.9	417	417
150	4.0358	6430	3163	781	279	748	17.0	416	416
175	4.0376	6417	3152	778	276	741	19.7	414	414
200	4.0397	6402	3137	774	273	733	21.9	412	412
225	4.0420	6383	3120	771	270	726	23.2	410	410
250	4.0444	6363	3101	767	266	716	23.7	407	407
275	4.0467	6340	3079	762	262	705	23.7	404	404
300	4.0489	6316	3057	757	258	696	23.7	401	401

Std. Dev. I.P. =  $0.1 \times 10^{-5}$  Åstd. Dev.  $v_L = 3.0$  Std. Dev.  $v_S = 0.7$  M/Sec

Table 3: Bulk modulus, shear modulus, young's modulus, coefficient of thermal expansion and Debye temperature of Aluminium - 2 percent zinc alloy determined through the least square fit of the measured data.

Temp °K	Lattice para.o (Å)	Velocity (Long.) M/sec	Velocity (shear) M/sec	Bulk Mod. k bar	Shear Mod. k bar	Young's Mod. k bar	Coeff. Th.exp. x10 <sup>6</sup> /K	Θ <sup>D</sup> °K calc.
0	4.0305	5384	3122	788	277	744	0.0	411
25	4.0305	5384	3121	788	276	743	1.2	411
50	4.0308	5382	3121	787	276	742	3.4	411
75	4.0313	5377	3119	786	276	742	6.4	410
100	4.0321	5370	3116	784	275	742	10.0	410
125	4.0332	5362	3111	782	274	737	13.7	409
150	4.0348	5352	3103	778	273	734	17.3	408
175	4.0367	5338	3093	775	270	730	20.4	407
200	4.0389	5323	3079	771	267	719	22.8	405
225	4.0412	5305	3061	768	264	711	24.2	402
250	4.0437	5285	3039	764	260	701	24.2	399
275	4.0460	5263	3011	761	255	688	24.2	395
300	4.0481	5238	2978	759	249	674	24.2	391

Std.Dev. L.P. =  $0.2 \times 10^{-2} \text{Å}$  Std. Dev.  $v_1 = 18.5 \text{ M/sec.}$  Std.Dev.  $v_g = 12.3 \text{ M/sec.}$

Table 35 : Bulk modulus, shear modulus, young's modulus, coefficient of thermal expansion and Debye temperature of Aluminium - 5 percent zinc alloy determined through the least square fit of the measured data.

Temp °K	Lattice para.o (A)	Velocity (Long.) M/sec	Velocity (shear) M/sec	Bulk Mod. k bar	Shear Mod. k bar	Young's Mod. k bar	Coeff. Th.exp. $\times 10^6$	$\theta_D^{\circ K}$ calc.
0	4.0295	6336	3099	788	277	744	0.0	408
25	4.0296	6336	3099	788	277	744	1.9	408
50	4.0299	6335	3097	787	275	742	4.4	408
75	4.0304	6331	3095	786	275	742	7.3	407
100	4.0314	6326	3090	785	275	740	10.4	407
125	4.0326	6318	3084	783	273	735	13.6	406
150	4.0340	6308	3075	780	272	732	16.6	405
175	4.0359	6296	3065	777	269	724	19.4	403
200	4.0380	6280	3050	774	266	717	21.7	401
225	4.0402	6262	3032	771	262	706	23.4	398
250	4.0426	6242	3008	767	258	697	24.2	395
275	4.0450	6220	2980	765	253	684	24.2	391
300	4.0474	6197	2945	763	247	669	24.2	387

Std. Dev. L.P. =  $0.2 \times 10^{-5}$  Å      Std. Dev.  $v_l = 1.1$  M/sec.      Std. Dev.  $v_s = 1.0$  M/sec.

Table 25 : Bulk modulus, shear modulus, young's modulus, coefficient of thermal expansion and Debye temperature of Aluminium 4 percent Zinc alloy determined through the least square fit of the measured data.

Temp °K	Lattice para.o (A)	Velocity (Long.) M/sec.	Velocity Shear M/sec.	Bulk Mod. k bar	Shear Mod. k bar	Young's Mod. k bar	Coeff. th.exp. x10 <sup>6</sup> /K	°K calc..
0	4.0289	6256	3059	789	277	744	0.0	403
25	4.0290	6255	3059	789	277	744	1.3	403
50	4.0292	6254	3058	789	277	744	3.6	403
75	4.0297	6250	3055	788	276	743	6.6	402
100	4.0305	6245	3050	786	275	740	10.0	402
125	4.0317	6237	3043	785	274	737	13.6	400
150	4.0332	6227	3033	783	271	729	17.1	399
175	4.0351	6215	3020	780	269	724	20.2	397
200	4.0373	6201	3005	777	266	717	22.7	395
225	4.0396	6184	2988	774	262	706	24.2	393
250	4.0421	6164	2969	769	258	697	24.5	390
275	4.0445	6142	2950	765	255	689	24.5	387
300	4.0466	6119	2930	759	251	679	24.5	385

Std.Dev.L.P.= $0.2 \times 10^{-5}$  Å      Std.Dev.v<sub>1</sub>=9.5 M/sec.      Std.Dev.v<sub>s</sub>=4.2 M/sec.

Table 37 : Bulk modulus, shear modulus, young's modulus, coefficient of thermal expansion and Debye temperature of Aluminium 10 percent Zinc alloy determined through the least square fit of the measured data.

Temp °K	Lattice para.o (Å)	Velocity (Long.) M/sec.	Velocity (Shear) M/sec.	Bulk Mod. k bar	shear Mod. k bar	Young's Mod. k bar	Coef. th.exp. x10 <sup>6</sup> /°K	60°K cal.
0	4.0282	6091	2900	797	259	701	0.0	383
25	4.0283	6089	2900	797	259	701	0.9	383
50	4.0285	6085	2900	795	259	701	3.0	382
75	4.0289	6079	2897	793	253	699	6.0	382
100	4.0297	6073	2891	792	257	696	9.6	381
125	4.0308	6065	2880	791	255	691	13.4	380
150	4.0324	6053	2865	789	252	684	17.0	378
175	4.0342	6037	2848	786	249	676	20.1	375
200	4.0363	6014	2831	780	245	666	22.4	373
225	4.0386	5980	2816	769	242	657	23.5	371
250	4.0409	5953	2808	752	241	654	23.5	369

Std.Dev.L.P.=0.1x10<sup>-5</sup> Å    Std.Dev. v<sub>l</sub>=4.7 M/sec.    Std.Dev.v<sub>s</sub>=7.5 M/sec.

Table 33 : Bulk modulus, shear modulus, young's modulus coefficient of thermal expansion and Debye temperature of Aluminium 15 per-cent Zinc alloy determined through the least square fit of the measured data.

Temp °K	Lattice para.o (Å)	Velocity (Long.) M/sec.	Velocity (Shear) M/sec.	Bulk Mod. k bar	Shear Mod. k bar	Young's Mod. k bar	coeff. of th. ex. $\alpha_{100}/^\circ\text{K}$	of $G/G_K$ calc.
0	4.0258	5856	2798	783	257	696	0	369
25	4.0258	5856	2797	783	257	696	0.5	369
50	4.0259	5856	2796	783	257	696	2.5	369
75	4.0263	5851	2793	782	256	693	5.7	369
100	4.0271	5844	2789	780	255	690	9.5	368
125	4.0282	5836	2783	778	254	638	13.6	367
150	4.0298	5824	2775	774	252	682	17.3	366
175	4.0317	5808	2764	769	250	677	20.3	364
200	4.0338	5787	2752	763	247	669	22.1	363
225	4.0360	5760	2738	755	244	661	22.7	360
250	4.0381	5727	2723	745	241	653	22.7	358

Std.Dev. L.P. =  $0.1 \times 10^{-5}$  Å, Std.Dev.  $v_1 = 5.6$  M/sec. Std.Dev.  $v_s = 4.4$  M/sec.

**Fig. 14** Temperature dependence of the longitudinal wave velocity in Al and Al - Zn alloy

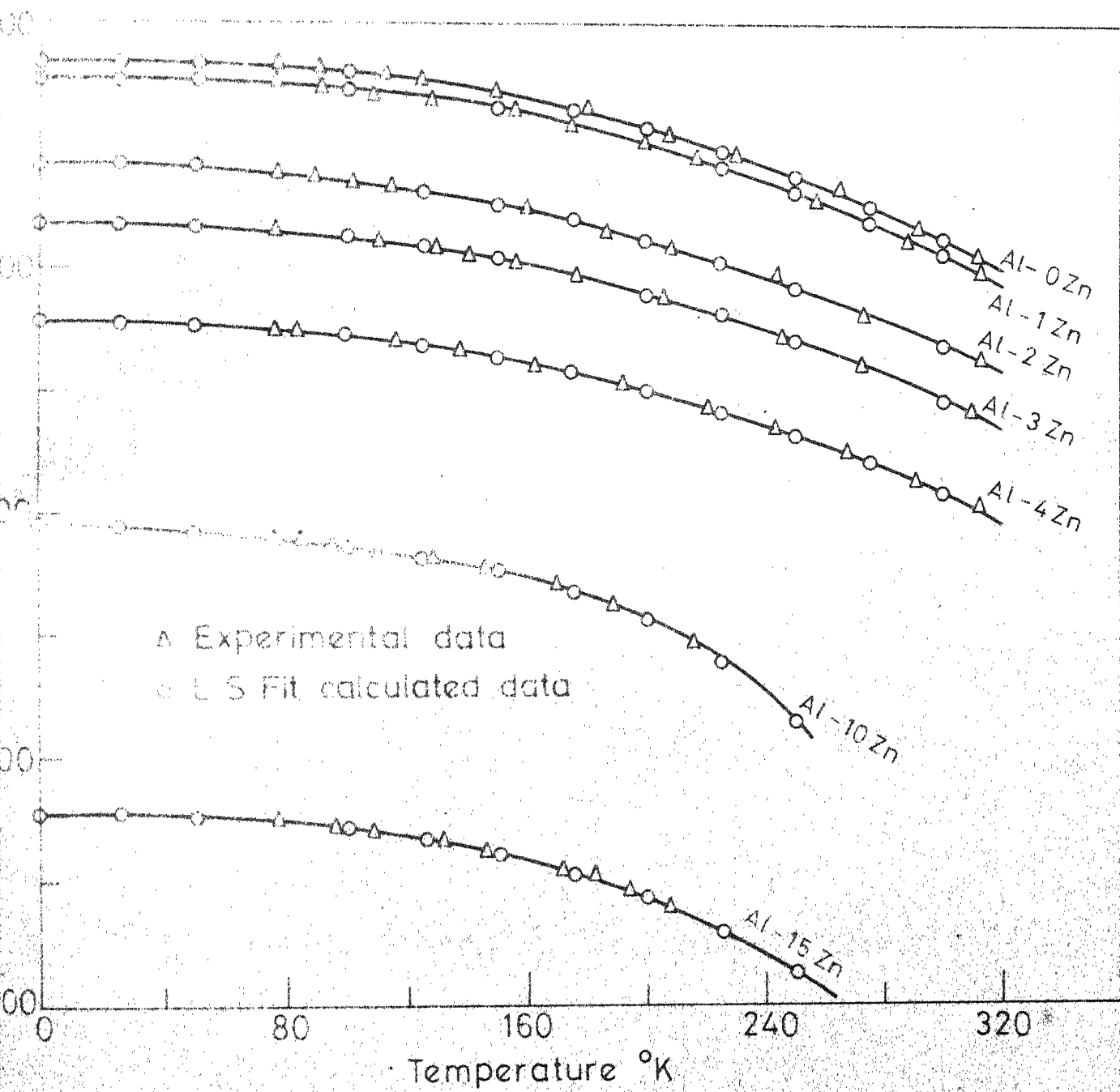


Fig. 14



**Fig. 15** Temperature dependence of the shear wave velocity in Al and Al - Zn alloy

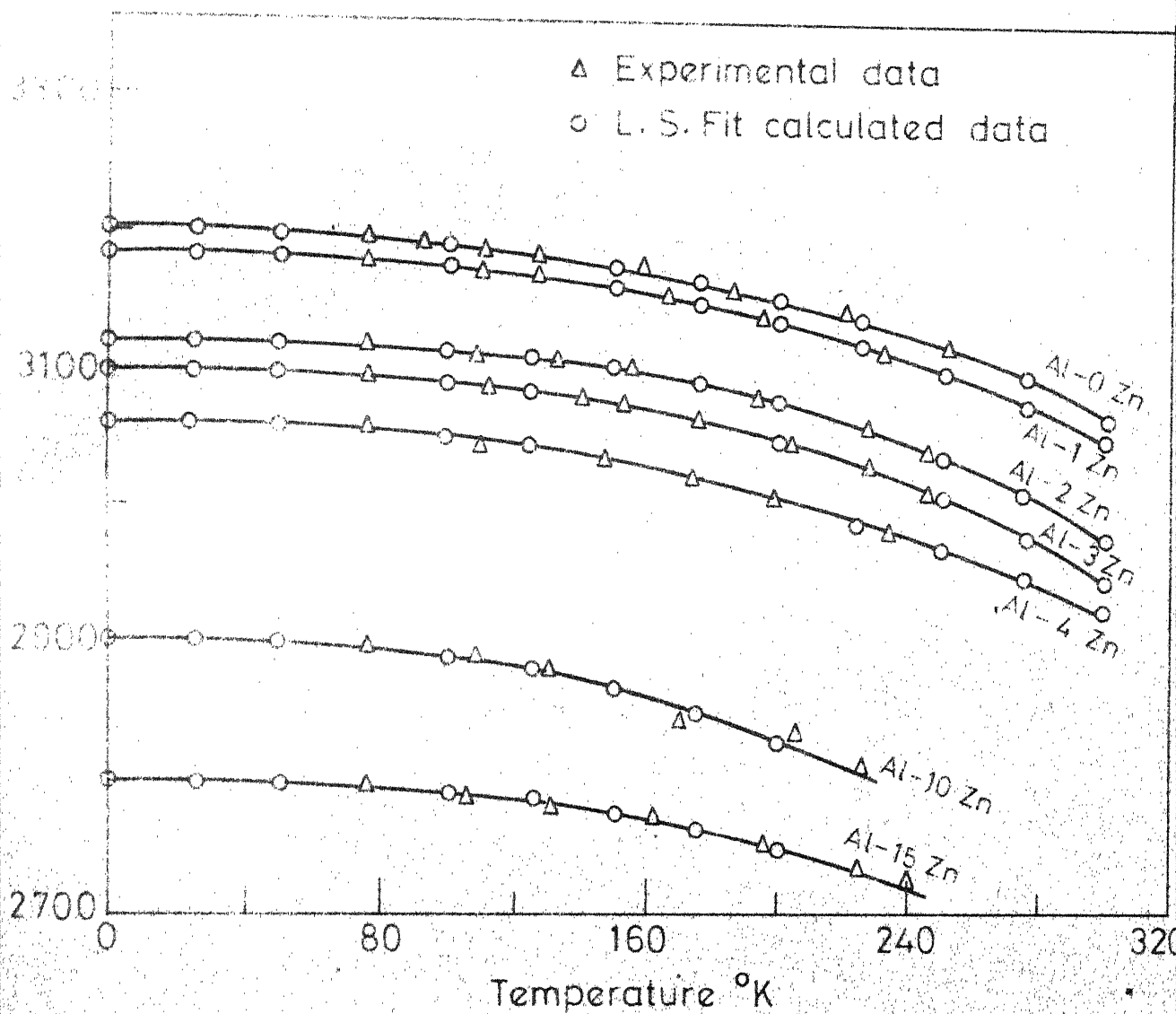


Fig. 15

**Fig. 16** Temperature dependence of the lattice parameters of Al - Zn alloy

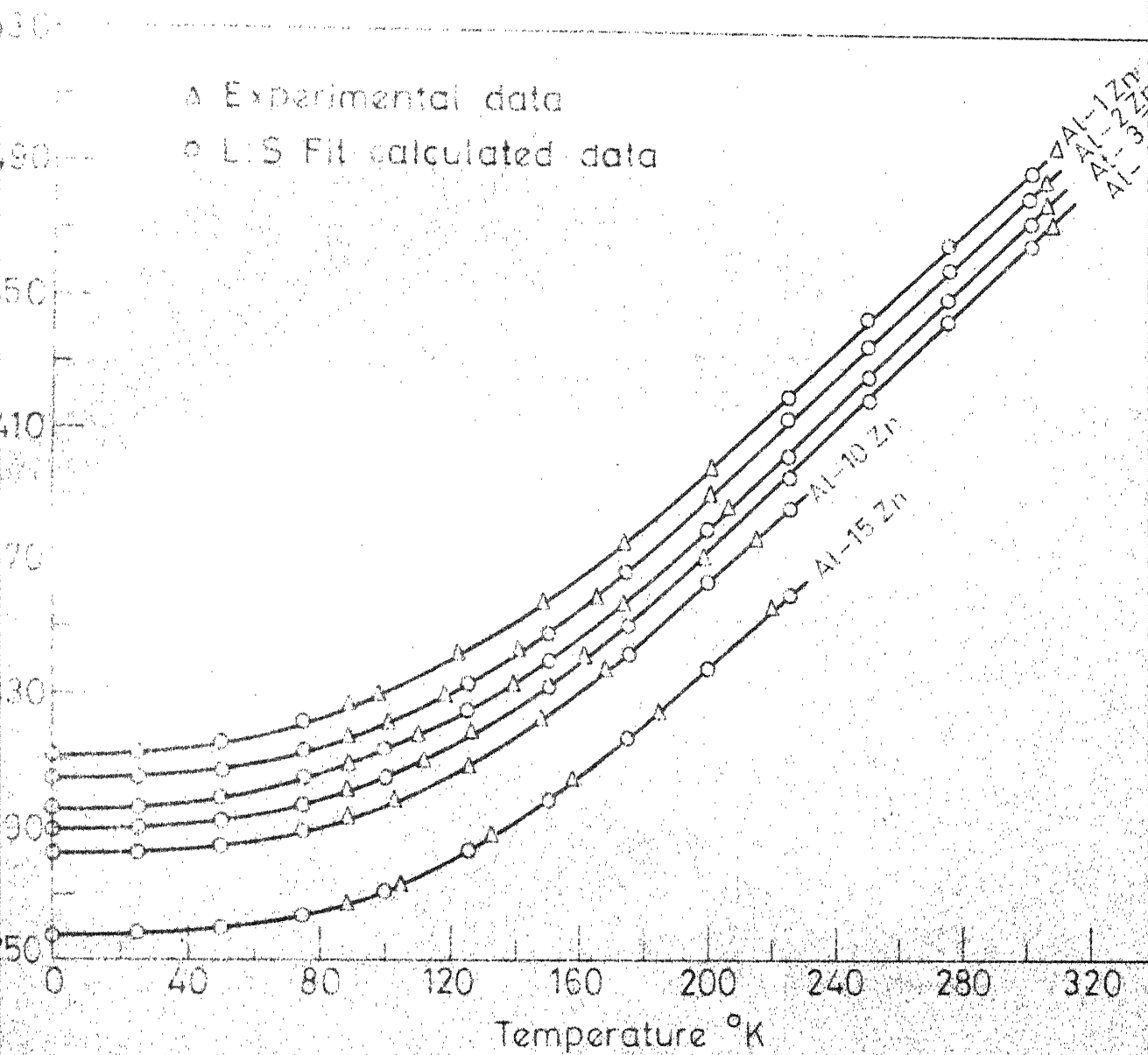


Fig. 16

**Fig. 17** Debye temperature of Al and Al - Zn alloy

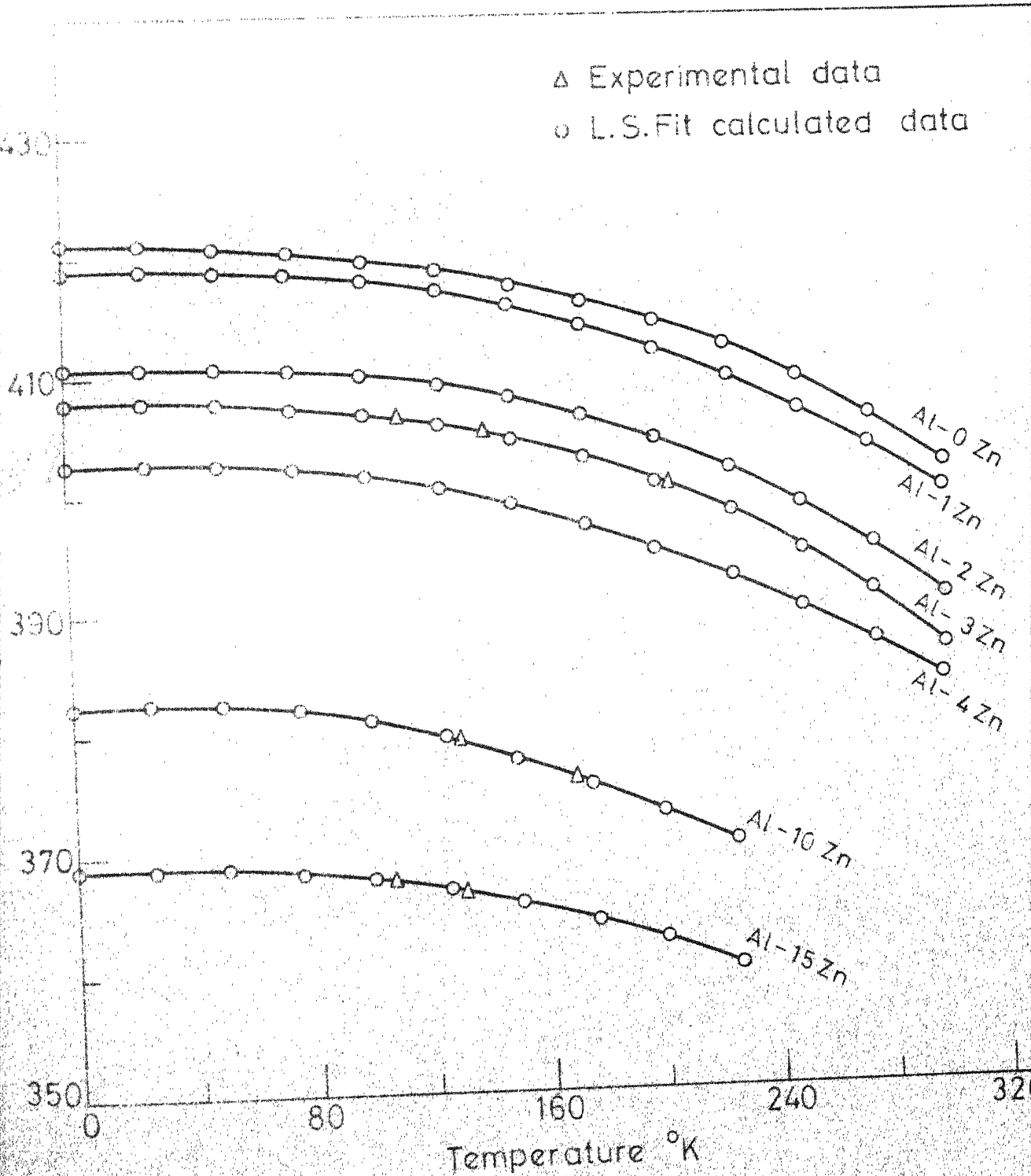


Fig. 17

**Fig. 18** Variation of the  $0^\circ\text{K } \Theta_D$ , bulk modulus and shear modulus as a function of atomic percent Zn

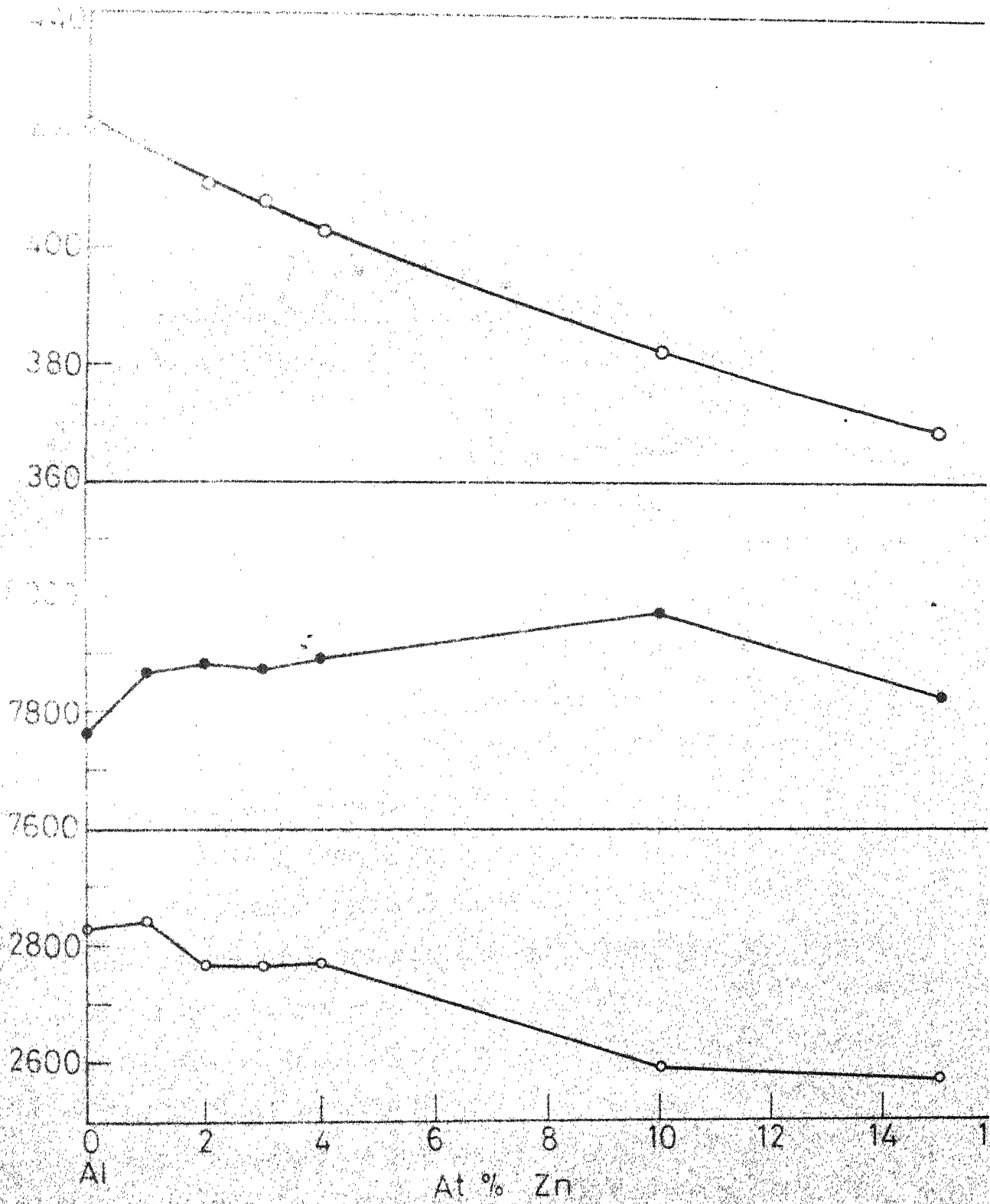


Fig. 18





## CHAPTER 6

### DISCUSSIONS

The performance of the pulse-echo equipment was tested by measuring the velocity of longitudinal waves in pure copper (99.99 pct.) at 77°K and 306°K (Table 5). Copper was specifically chosen for this purpose because the reported values of the single - crystal elastic moduli of copper from various sources<sup>54-56</sup> were very close to each other. No data in the required temperature range (77°K to 300°K) was available for polycrystalline specimens of copper. In order to compare the observed velocities, the single crystal elastic moduli of copper reported by Overton and Gaffney<sup>54</sup> was converted to an averaged velocity of longitudinal waves for polycrystalline specimens using the VRH method<sup>61</sup> (Table 5). The work of Overton and Gaffney was chosen for this purpose because the single - crystal elastic moduli for copper between 0°K and 300°K has been reported and values at 77°K and 306°K could be easily found by interpolation and extrapolation. The accuracy of the single crystal data was reported to be 1.8 pct. i.e. about 90 M/sec in terms of the longitudinal velocity. In the present investigation longitudinal wave velocity in polycrystalline specimens of copper has an accuracy of about 40 M/sec. According to Table 5, the differences

between the observed and calculated velocities are 53 and 36 M/sec, respectively, at 77°K and 306°K. The small difference between the calculated and measured velocities are well within the total error limit and thus indicates that the present measurements are reliable.

The measured longitudinal and transverse wave velocities for pure aluminium at 0°K was found to be 6468 and 3204 M/sec. (Table 30). Anderson<sup>62</sup> calculated the average velocity of the longitudinal and transverse ultrasonic waves at 0°K from the measured single crystal elastic moduli<sup>9</sup> to be 6794 M/sec and 3235 M/sec respectively. While the measured velocity of shear waves match well with Anderson's data the measured value of the longitudinal velocity is about 5 pct. lower than the calculated value. This may be due to the fact that considerable difference exists among the single crystal elastic moduli of Al reported by various workers<sup>9,54</sup>. Using the data of Schmunk and Smith<sup>65</sup> at 298°K Anderson<sup>66</sup> calculated the average longitudinal and shear wave velocity and reported them to be 6422 M/sec and 3110 M/sec respectively. Kar et al<sup>67</sup> used the third order elastic moduli of Al at room temperature measured by Sarma and Reddy<sup>68</sup> and Thomas<sup>69</sup>. The results of the present investigation show the velocities to be

6324 and 3065 M/sec. Agreement of the calculated wave velocities at 298°K with the present data is better than that at 0°K. Longitudinal wave velocities in single and polycrystalline specimen of pure Al has been measured at room temperature by Rokhlin<sup>28,29</sup> at room temperature (not mentioned) and in both the cases the longitudinal wave velocity was found to be about 6300 M/sec.

In spite of the wide use of Al-Zn alloys as good sound conductors<sup>51,52</sup>, little established data exists on the ultrasonic behaviour of these alloys. Rokhlin<sup>28,29</sup> reported a general effect of Zn addition to the longitudinal and transverse wave velocity of polycrystalline specimens and on the longitudinal wave velocity in single crystals of Al at room temperature. Using Annealed specimens with Zn content upto about 15 at. pct. he showed a linear decrease in longitudinal wave velocity from about 6300 M/sec in case of pure Al to about 5600 M/sec in case of Al<sub>85</sub> Zn<sub>15</sub> alloy. Similarly, the shear wave velocity was found to decrease from about 3100 M/sec to about 2700 M/sec.

The measured velocities of longitudinal and shear waves in six Al-Zn alloys between 0°K and 300°K indicate, as in Rokhlin's work, that addition of Zn to Al the ultrasonic wave velocities decrease at all temperatures. A

comparison of the present results with the work of Rokhlin is, however, possible only upto a Zn content of 4 at. pct. Zn since beyond that concentration the specimens used in the present work (10 at.pct. Zn and 15 at. pct. Zn) were in the quenched single phase state and specimens with similar composition in Rokhlin's work were in the annealed and two phase state. For the alloy  $\text{Al}_{96}\text{Zn}_4$  the longitudinal and shear wave velocities at room temperature ( $300^\circ\text{K}$ ) is 6119 M/sec and 2930 M/sec. (Table 35) and the values corresponding to the same composition from Rokhlin's work are about 6100 M/sec and 3000 M/sec. respectively, in very good agreement.

A comparison of the effect of further addition of Zn to Al on the velocities in the present investigation may be made with Rokhlin's<sup>28,29</sup> work. His data, however, is with annealed specimens and at room temperature. Considering the values at  $0^\circ\text{K}$ , as obtained in this work, the longitudinal and shear wave velocities for the alloys  $\text{Al}_{90}\text{Zn}_{10}$  and  $\text{Al}_{85}\text{Zn}_{15}$  went down to 6091 M/sec, 2900 M/sec 5856 M/sec and 2798 M/sec, with respect to the values for pure Al. The reduction in the velocities per at. pct. Zn. is comparable to the same parameter at room temperature reported by Rokhlin.

Lattice parameter of pure Al has been determined by a number of workers. Table 39 summarises some of these and a comparison with the present work is made. It is to be noted that there exists some observable difference in the reported lattice parameter of high purity Al at room temperature<sup>70-73</sup>. Data for the present work is close to that of Dorn et al<sup>70</sup>.

The above test was performed at room temperature and it was also important to test the performance of the attachment at intermediate temperatures between 77°K and 300°K. The same Al powder was used for testing at low temperatures. Lattice parameter was measured at a few temperatures between 89°K and 200°K. Thermal contraction data ( $\Delta l/l_0$ ) obtained by dial gauge dilatometer<sup>73</sup> and by interferometric method<sup>74</sup> was used for calculating the expected lattice parameters at low temperatures on the basis of the measured lattice parameter at 306°K, which agreed well with several other data. The comparison of the observed and the published data given in Table 39 shows a very good match. At low temperature agreement with Figgin's<sup>73</sup> data is noticeable, but considerable difference with that of Heumann's<sup>75</sup> exists.

Variation of the lattice parameter of Al-Zn alloys with temperature is shown in Fig. 16. The general trend

Table 39 : Lattice Parameter of Al from various sources

Temp °K	Lattice Parameter $\overset{\circ}{\text{\AA}}$	Purity	Reference
0	4.0236	-	68
0	4.0315	99.9	X
75	4.0327	99.99	73
75	4.0325		X
100	4.0334	99.9	X
100	4.0334		X
125	4.0353	99.99	73
125	4.0347	99.9	X
150	4.0365	99.9	+74
150	4.0363		X
223	4.0427	99.994	69
225	4.0426	99.9	X
225	4.0415		+ 74
298	4.0495	99.995	72
298	4.0494	99	70
298	4.0496	-	71
298	4.0497	99.99	73
300	4.0494	99.9	X

X Least square polynomial fit curve data points (Table 32)

+ Room temperature data of the present work used with thermal contraction data of Nix and McNair.

in the alloys is similar to that of pure Al. It is observed that addition of Zn caused a monotonic reduction in the lattice parameter. Comparison can be made with the work of Dorn et al.<sup>70</sup> and Axon and Hume-Rothery<sup>72</sup>. For the alloy  $\text{Al}_{99.25}\text{Zn}_{0.75}$  Dorn reported a lattice parameter of 4.0489 Å at 298°K while in the present work the same parameter was observed for  $\text{Al}_{99}\text{Zn}_1$  at 300°K (Table 33). For the alloys  $\text{Al}_{98.3}\text{Zn}_{1.7}$  and  $\text{Al}_{97.1}\text{Zn}_{2.9}$  Axon and Hume-Rothery<sup>72</sup> reported lattice parameters of 4.0484 Å and 4.0476 Å, respectively, while in the present work the parameters for  $\text{Al}_{98}\text{Zn}_2$  and  $\text{Al}_{97}\text{Zn}_3$  at 300°K are 4.0481 Å and 4.0474 Å, respectively (Tables 34 and 35).

Thermal expansion coefficients for all the specimens at 25°K intervals have been calculated from the polynomial fit of the experimental data and are shown in Tables 32 to 38. According to the present data the thermal expansion coefficient for Al at 300°K is  $23.2 \times 10^{-6}$  per °K. It compares well with the room temperature data of Straumanis and Iovene<sup>71</sup>, which is  $23.3 \times 10^{-6}$  per °K and of Nix and McNair<sup>72</sup>, which is  $23.6 \times 10^{-6}$  per °K. In case of the alloys a slight increase in the coefficient with increasing Zn content has been observed (Tables 32 - 36). For the alloys with 1, 2, 3 and 4 at. pct. Zn, the coefficient at 300°K is found to be  $23.7 \times 10^{-6}$ ,  $24.2 \times 10^{-6}$ ,  $24.2 \times 10^{-6}$  and  $24.5 \times 10^{-6}$  per °K.



These values do not agree well with those of Hume Rothery and Baultbee<sup>76</sup> even though they indicated increasing trend.

Fig. 17 shows the pattern of the variation of  $\Theta_D$  with temperature for all the specimens. The general trend is normal, in the sense that a monotonic reduction in  $\Theta_D$  is observed. In a few alloys of  $v_1$ ,  $v_s$  and  $a_0$ , were measured almost at the same temperatures (Table 40) and direct calculation of  $\Theta_D$  without the polynomial fit was possible. These directly calculated data points are shown in Fig. 17 which match very well with the curves drawn on the basis of the polynomial fit. Thus, it may be inferred that the approximation associated with the L.S. Fit was very nominal and the method of estimation of  $\Theta_D$  is dependable.

Debye temperature of the specimens at different temperatures are given in Tables 32 to 38. In case of pure Al,  $\Theta_D$  decreases from 421°K at 0°K to 402°K at 300°K. Debye temperature at 0°K from various sources are given in Table 41. From the table it is observed that the values of the Debye temperature for Aluminium are scattered over a range of temperature. The present data, 421°K, obtained with a polycrystalline specimen is in reasonable agreement with the more recent thermal and elastic ones. The accuracy

Table 18 : Debye temperature of some Al-Zn alloys calculated from the measured values.

Specimen composition	Observed Quantity	Observed Value	Temp. of observation	$\Theta_D$ °K
Al-3Zn	Velocity(L)	6326 M/sec	113	406
	Velocity(S)	3088 M/sec	112	
	L.P.	4.0318 Å	110	
	Velocity(L)	6311 M/sec	140	405
	Velocity(S)	3079 M/sec	141	
	L.P.	4.0335 Å	139	
	Velocity(L)	6293 M/sec	177	403
	Velocity(S)	6063 M/sec	177	
	L.P.	4.0357 Å	174	
	Velocity(L)	6278 M/sec	206	400
	Velocity(S)	3047 M/sec	205	
	L.P.	4.0386 Å	207	
Al-10Zn	Velocity(L)	6066 M/sec	129	379
	Velocity(S)	2882 M/sec	130	
	L.P.	4.0307 Å	125	
	Velocity(L)	6042 M/sec	170	376
	Velocity(S)	2842 M/sec	170	
	L.P.	4.0337 Å	168	
Al-15Zn	Velocity(L)	5842 M/sec	108	368
	Velocity(S)	2786 M/sec	106	
	L.P.	4.0273 Å	105	
	Velocity(L)	5837 M/sec	131	367
	Velocity(S)	2780 M/sec	131	
	L.P.	4.0287 Å	133	

Table 41 : Debye Temperature of Al from Various Sources

Debye Temperature °K	Method of Measurement	Reference
380	Thermal	85
390	"	86
418	"	87
427	Elastic	22
427	"	88
428	Thermal	89
431	Elastic	54

associated with the present data is about 1 pct. Within this limit of experimental error there is good agreement and it may be said that the use of the simple method of using polycrystalline specimens for the estimation of  $\Theta_D$  is quite dependable. Particularly in case of alloys where single crystals may not be grown easily, a check on the sp.heat data can always be made in this way.

Fig. 18 shows the variation of  $\Theta_D$ , Bulk modulus and shear modulus of the specimens with Zinc content. The variation of  $\Theta_D$  is very smooth and continuously decreasing with increasing Zn content. The variation in case of the moduli is very small. However, a monotonic decrease in the shear modulus can be observed. No clear trend is found in case of the bulk modulus, which is found to increase to a maximum at 10 at. pct. Zn and then decrease. For pure Al the standard values for the Bulk modulus, Young's modulus and the shear modulus are 752, 706 and 262 Kbars respectively at room temperature<sup>90</sup>. This compares quite well with the observed values, i.e. 748, 690 and 256 Kbars respectively (Table 32).

Very few simple alloy systems have been studied by the ultrasonic pulse - echo technique to determine the wave velocities or the elastic moduli as a function of composition. Still less data is available on the variation

of  $\Theta_D$  at 0°K with solute content. Koster and Rauscher<sup>78</sup> reported the variation in Young's modulus with composition of some Cu base alloys. Zener<sup>79</sup> explained the same data<sup>78</sup> from the size effect point of view. Cabarat et al<sup>80</sup> and Smith<sup>81</sup>, like Koster and Rauscher indicated a linear drop in the Young's modulus with solute content. Smith<sup>81</sup>, drawing similarity from the variation of the solidus with alloying element suggested that the Young's modulus was directly proportional to the electron-atom ratio. The theoretical work on the elastic constants of copper was done by Fuchs<sup>77</sup>. Smith and his coworkers<sup>82,83</sup>, through a semi-empirical approach based on Fuch's work, has been able to show that the variation of single crystal shear moduli with composition is strongly dependent on  $Z$ , the number of average charge per ion, and  $\alpha$ , which is a measure of the decrease in the number of closed shell repulsions per added impurity. Unlike the analysis of Koster and Rauscher<sup>78</sup>, Zener<sup>79</sup> and Smith<sup>81</sup>, the analysis of Smith and coworkers needs the single crystal shear moduli.

The variation of  $\Theta_D$  at low temperatures with composition for some Cu alloys is available through the sp-heat and elastic constants measurements. Mizutani et al<sup>84</sup>, through sp-heat measurements of Cu and Ag alloys with Ge, Ga, In etc

showed that,  $\Theta_D$  decreases with increase in solute content.

$\Theta_D$  calculated from single crystal elastic constants of Cu-Zn alloys<sup>54</sup> supports Mizutani et al's finding. Cain and Thomas<sup>26</sup> measured single crystal elastic constants of  $\alpha$  Cu-Al alloys. They found that the elastic constants decrease with increasing solute content whereas  $\Theta_D$  increased. The polycrystalline elastic moduli of Cu-Al alloys measured by Linkhery and Lahteenkorva<sup>25</sup> also support Cain and Thomas's work. Unlike the attempts to explain the change in the elastic moduli with composition, no attempt so far has been made to explain the change of  $\Theta_D$  with composition.

Pettrell<sup>91</sup> has used simple arguments to indicate the relation between frequency (and hence  $\Theta_D$ ), lattice parameter ( $a$ ), mass (or density) and Young's modulus ( $Y$ ) through the relation

$$\text{frequency} \propto Y a \left( \frac{1}{n} \right)^{\frac{1}{2}}$$

where  $n$  is atomic mass. This relation may serve as a qualitative indication of the nature of variation of  $\Theta_D$  with composition.  $\Theta_D$  will decrease when  $Y$  and  $a$  decrease and  $n$ , which is the average atomic mass in the alloy, increases with composition. Similarly, if  $Y$  and  $a$  increase and  $n$  decreases

with composition  $\Theta_D$  will increase. For the intermediate cases, i.e. when  $Y$  and  $n$  vary in opposite manner with composition and  $n$  increases or decreases, the variation of  $\Theta_D$  will be influenced by the factors strongly dependent on composition. In the case of Cu-Al alloys,  $n$  is expected to decrease rapidly with increase in Al content and  $a$  is known to increase. The variation of  $Y^{25}$  with composition is not large. Hence,  $\nu$  (and  $\Theta_D$ ) is expected to increase. For other copper alloys with the solute from the same long period as copper,  $n$  does not vary rapidly and hence  $\Theta_D$  is expected to be dependent on the stronger of the factors between  $Y$  and  $n$ .

In the present case of Al-Zn alloys  $Y$  decreases,  $a$  decreases and  $n$  increases. Hence,  $\Theta_D$  is expected to decrease. It is known that elastic moduli are dependent on electron concentration. The present data, however, is not sufficient to establish the dependence of  $\Theta_D$  on electron concentration.

The qualitative justification that the decrease in  $\theta_D$  with increase in Zinc content in Al is due to decrease in  $a$  and increase in  $m$ , i.e. due to increase in density, also finds support from the theoretical work of Leigh on Al<sup>92</sup> and Al alloys<sup>93</sup>. Since the shear constants  $\frac{1}{2}(C_{11}-C_{12})$  and  $C_{44}$  are proportional to the second derivative of the total energy of a crystal with respect to strain parameters, Leigh like Fuchs<sup>77</sup>, has first identified the contributions to the total energy of on Al crystal. He has shown that the two terms which are important in estimating shear constants of Al are the purely electrostatic energy terms and the Fermi Energy. The contribution to the shear constants due to the electrostatic energy term is highly anisotropic but the measured shear constants of Al indicate that Al is more or less isotropic. Leigh<sup>92</sup> considered that the isotropic behaviour of Al is due to a suitable negative contribution due to Fermi Energy. Since Al is trivalent and the first Brillouin zone of fcc metal can accommodate two electrons per atom, a zone overlap occurs in the case of Al. The first Brillouin zone for Al is bounded by hexagonal and cube faces. Using the measured shear constants<sup>94</sup> Leigh has shown that there must be overlap across the hexagonal as well as the cube faces. The overlapping electrons give rise to a large negative contribution to one of the shear constants (See Table 41) so that the effective shear constants of Al become more or less equal.



Table 42 : Contributions to shear constants calculated by Leigh<sup>92</sup>

Contributed to from	$\frac{1}{2}(C_{11}-C_{12})$ Dynes/cm <sup>2</sup>	$(C_{44})$ Dynes/cm <sup>2</sup>
Coulomb interaction	1.3	11.4
First zone electrons	1.5	4.5
Overlapping electrons	-0.7	-13.05
Total	2.1	2.85
Measured values <sup>94</sup>	2.085	2.853

When Al is alloyed with an element of lower valency, there is a decrease in the number of electrons per atom and hence the effect of alloying Al with lower valent element will be to decrease the number of electrons in the second zone. Since this decrease in the number of electrons leads to a decrease in the number of electrons across the cube faces of the zone boundary (electrons across the cube faces have higher energy than those across the hexagonal faces) the shear constant  $\frac{1}{2}(C_{11}-C_{12})$  increase with an increase in solute content, and goes through a maximum at  $e/a = 2.67$  at which the cube face overlap vanishes. The other shear constant,  $C_{44}$ , begins to increase appreciably only after further increase in solute content takes place, i.e. when the number of electrons across the hexagonal faces begins to decrease. Leigh<sup>93</sup> has calculated the shear constants of Al-Zn alloys. Using these elastic constants to estimate the modulus of rigidity  $G$ , Eqns. 16, 17 and 18 and assuming that the bulk modulus  $K$  remains a constant on alloying Leigh has

has evaluated  $\Theta_D$  of Al-Zn alloys which is shown in Fig. 19 as a function of Zn content. It is clear from Fig. 19 and Eqs. 16, 17 and 18 that initially a decrease in  $\Theta_D$  is expected with an increase in Zn content and this decrease is primarily due to the increase in density as Al is replaced by Zn. (See the dashed curve in Fig. 19 which is due to a change in only i.e., with  $K$  and  $G$  assumed to be constants). The effect of the increase in  $\Theta_D$  with increase in shear constant  $\frac{1}{2}(C_{11}-C_{12})$  become effectively only above about 20 at pct Zn; beyond the composition range of investigation. The calculated  $\Theta_D$  values of Leigh connect be compared with the present results because many simplifying assumptions were made in theoretically evaluating  $\Theta_D$ . The decrease of  $\Theta_D$  with increasing Zn content, however, match quite well with the present result. The relative decrease of the calculated  $\Theta_D$  value from Al-15 at pct Zn is very close to what has been observed ( 50°K) in the present investigation.

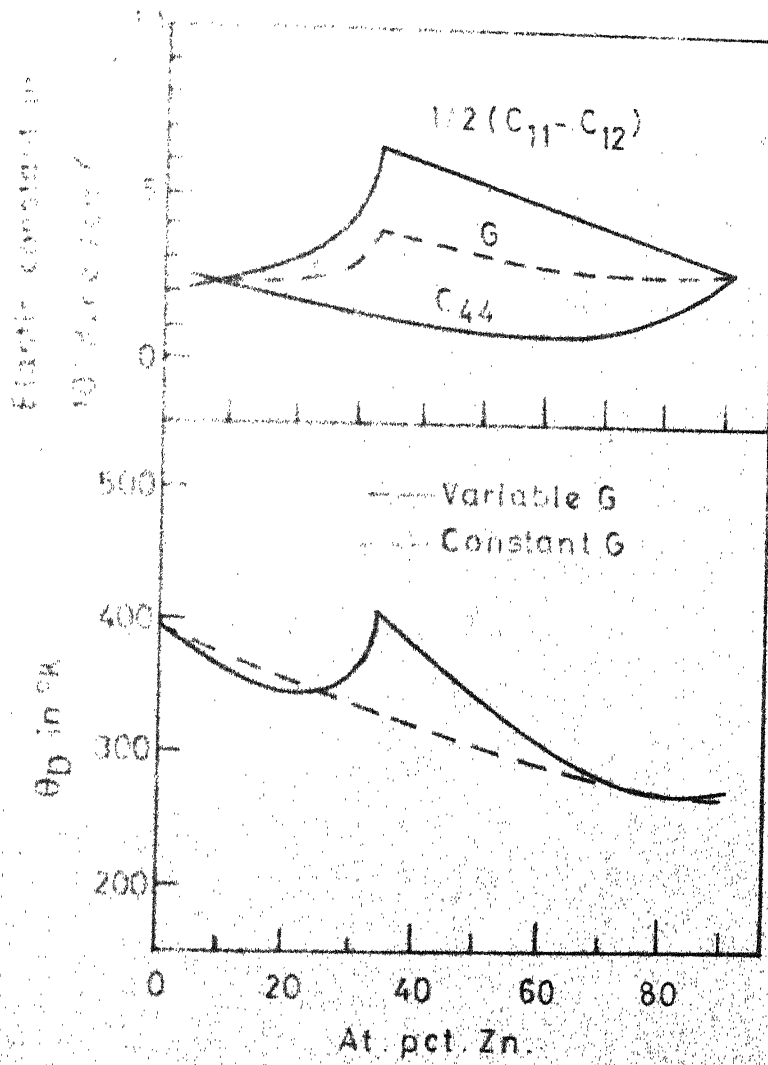


FIG. 19

## CHAPTER 7

## CONCLUSIONS

1. Velocities of longitudinal and shear ultrasonic waves in a polycrystalline Al specimen is close to the calculated average value obtained by VRH approximation of the data from single crystal measurements. Debye temperature ( $\Theta_D$ ) calculations for Al based on the observed velocities in a polycrystalline specimen show very good agreement with the  $\Theta_D$  obtained from single crystal data.
2. With addition of Zn to Al, both the longitudinal and shear wave velocities in the alloys decrease continuously.
3. With addition of Zn to Al, the lattice parameter of  $\alpha$ -phase quenched alloys measured below 250°K was found to decrease continuously.
4. With addition of Zn to Al, the polycrystalline shear modulus and Debye temperature at 0°K shows a systematic decrease but the bulk modulus increases slightly upto about 10 at.pct.Zn and then decreases. Young's modulus, calculated from bulk modulus and shear modulus values also showed a decreasing trend with increasing Zn content.

5. The present data was insufficient to deduce the actual effects of alloying on the Debye temperature. The data qualitatively supports the idea that the decrease in  $\Theta_D$  with alloying is connected with the increase in the average atomic mass, and decrease in the lattice parameter and Young's modulus.

## REFERENCES

- [1] Russell, N., Gupta, K.P., Cheng, C.H., and Beck, P.A.  
J. Phys. Chem. Sol. 25, 993, (1964).
- [2] Einstein, A. Ann. Phys. Lpz. 22, 180, (1907).
- [3] Born, M. and Von Karman, Th. Phys. Z 13, 297 (1912).
- [4] Debye, P., Ann. Phys. Lpz. 39, 789 (1912).
- [5] Born, M. 'Atom theorie des festen Zustandes Lpz',  
(1923).
- [6] Musgrave, M.J.P. Proc. Roy, Soc. A 226, 339 (1954).
- [7] Kittel, C. 'Introduction to Solid State Physics',  
John Wiley and Sons, Ed. 3 (1968), p. 121.
- [8] Alers, G.A. 'By Physical Acoustics', V III B (Ed.  
W.P. Mason) Academic Press (1965) p. 7.
- [9] deLaunay, J., J. Chem. Phys. 22, 1676 (1954).  
24, 1071 (1956).
- [10] Marcus, P.M. (1960) Ref. of private communication in  
Ref. 8.
- [11] Hopf, J. and Lechner G. Verhandl. Deut. Physik Ges.  
16, 643, (1914).
- [12] Quinby, S.L. and Sutton, P.M. Phys. Rev. 91, 1122  
(1953).
- [13] Bhatia, A.B. and Tauber, G.E. Phil. Mag. 46, 108,  
(1955).
- [14] Betts, D.D. et al Phys. Rev. 104, 37, (1956).
- [15] Fedorov, F.I., Soviet Phys. Crystallography.  
8, 159 (1963)  
10, 125 (1965).

- [16] Fedorov, F.I., and Bystrova, T.G. Soviet Phys. Crystallography. 11, 333, (1966).
- [17] Kanti, L. and Varshni, V.P. Can. J. Phys. 47, 2022, (1969).
- [18] Voigt, W. Lehrbuch der Kristall Physik Lpz. p. 962, (1910).
- [19] Reuss, A. Angew Math. u Mech. 9, 49, (1929).
- [20] Hill, R.W. Proc. Phys., Soc. (London) A65, 349, (1952).
- [21] Gilvary, J. Phys. Rev. 103, 1701, (1956).
- [22] Anderson, O.L., J. Phys. Chem. Sol. 24, 910 (1963).
- [23] Featherstone, F.F. and Neighbours, J.R. Phys. Rev. 130, 1324, (1963).
- [24] Bernstein, B.J. J. App. Phys. 33, 2140, (1962).
- [25] Leukhery, J.T. and Lakteenkorva, E.E. Journal of Physics F.3, 1781, (1973).
- [26] Cain, L.S. and Thomas, J.F., Phys. Rev. B4, 4245, (1971).
- [27] Monent, R.L. J. App. Phys. 43, 4419, (1972).
- [28] Rokhlin, L.L. and Shirkov, V.S., Phys. of Met. and Metallurgy 36, 71, (1973)
- [29] Rokhlin, L.L. Soviet Phys. Acoustics 17, 224, (1971).
- [30] Voigt, W. Lehrbuch der Kristalphysik Lpz.p.716 (1928).
- [31] Fine, M.E., A.S.T.M. Bull. 181, 20, (1952).
- [32] Wegel, R. and Walther, M. Physica. 6, 141, (1935).
- [33] Bordoni, P.G., Nuovo Cimento 4, 177, (1947).
- [34] Pursey, H. and Pyatt, E.C. J. Sci. Instr. 31, 248, 1954.

- [35] Bhagwanan, S. and Bhimseshachar, J. Proc. Ind. AC. 28, 122, 928 (1944)
- [36] Bragg, D.L. J. App. Phys. 21, 941, (1950).
- [37] McKinnin, H.J., J. App. Phys. 24, 988, (1953).
- [38] Aaron, R. and Smith, C.S. Acta, Met. 4, 337 (1956).
- [39] deKlerk, J.D. and Musgrave, M.J.P., Proc. Phys. Soc. London, B68, 81, (1955).
- [40] Balaf, D.L. and Menon, M., J. App. Phys. 31, 1010, (1960).
- [41] Viswanathan, R. Ind. J. Phys. and App. Phys. 2, 53, (1964).
- [42] Mason, W.P. and Bommel, H.E., J. Ac.Soc.Am. 36, 644, (1956).
- [43] Blum, R.J. Rev. Sci. Instr, 34, 1400, (1963).
- [44] H. J. Mason, H.J., Physical Acoustics (Ed. W.P. Mason) Academic Press V I A p. 272.
- [45] Balaf, D.L. and deKlerk, J.D., I.E.E.E. Trans. Ultrasonic Engg UE 10, 27, (1963).
- [46] Brillouin, Z. Ann. Phys. 17, 88, (1922).
- [47] Chandrasekhar, V. Proc. Ind. Acad. Sc. 32A - 379, (1950).
- [48] Flubacher, P. et. al. J. Phys. Chem. Sol. 12, 53, (1959).
- [49] Ramakrishnan, G.N. and Wooster, W.A. Acta, Cryst, 4, 335, (1951).
- [50] Prince, E. and Wooster W.A. Acta, Cryst. 6, 450, (1953).
- [51] Davidson, S. Ultrasonics 3, 136, (1965).
- [52] May, J.D. Physical Acoustics (Ed. W.P. Mason) V I A Academic Press (1965).
- [53] Si, S.K. and Gupta, K.P., Trans. Ind. Inst. of metals 27, 267 (1974).



- [54] Rayne, J.A. Phys. Rev. 115, 62 (1959).
- [55] Overton, W.C. and Gaffney, J., Phys. Rev. 98, 969, (1955).
- [56] Waldorf, D.L. Phys. Chem. Sol., 16, 90 (1960).
- [57] Grubert, E and Joullie, A.M. Phys. Stat., Sol., 39, 357 (1970)
- [58] Ari, V., Wilson, J.H., Winrich, L and Sikora, P. Cryogenics 2 230 (1962).
- [59] Hansen, M, Constitution of Binary Alloys (McGraw-Hill) 1958, p. 149.
- [60] Panseri, C and Federight, J. Acta, Met. 8, 217, (1960).
- [61] Huntington, H.B., 'The Elastic Constants of Crystals', Academic Press, (1958), p. 113.
- [62] Parkin, L.S. and Gurry R.W., Thermodynamics of Metals (McGraw-Hill), Ch. VII.
- [63] Neighbours, J.R., Bratten, F.W., Smith, C.S., J. Appl. Phys. 23, 389, (1952.)
- [64] Smith, C.S. and Burns, J.W., J. Appl. Phys. 24, 15, (1953).
- [65] Schunk, R.E. and Smith, C.S., JPCS. 9, 100 (1959).
- [66] Anderson, O.L., Physical Acoustics Vol. III B, (Ed. W.P. Mason) Acad. Press, 1965, p. 44-84.
- [67] Kar, S.K., Misra, P.K. and Tandon, U.S. Sol. St. Comm. 15, 500, (1974).
- [68] Sarma, V.P.N, and Reddy, P.J. Phys. Stat., Sol. (A) 10, 563, (1972).
- [69] Thomas, J.F, (Junior) Phys. Rev. 175, 955, (1965.)
- [70] Dorn, J.E., Pietrokovsky, P. and Tietz, T.E. J. Metals, 2, 933 (1950).

- [71] Straumanis, M. and Ievins A. Z. Anorg, Chem. 238, 175 (1938).
- [72] Axon, H.J. and Hume-Rothery, W. Proc. Roy. Soc. A193, 1 (1948).
- [73] Figgins, B.F., Jones, G.O. and Riley, D.P. Phil. Mag. 8(1) 747, (1956).
- [74] Nix, F.C. and McNair D. Phys. Rev. 60, 597 (1941).
- [75] Heumann, T. Naturwiss. 32, 296 (1944).
- [76] Hume-Rothery, W and Boulton, T.H. Phil. Mag. 40, 71 (1949).
- [77] Fuchs, K. Proc. Roy. Soc (London) A151, 585 (1935), A153, 622 (1936), A157, 444 (1936).
- [78] Koster, W and Rouscher, Z. Metall, 39, 111, (1948).
- [79] Zener, C. Acta Cryst. 2, 163, (1949).
- [80] Cocharat, R., Guillet, L. and LeRoux, R. J. Inst. Met. 75, 391 (1949).
- [81] Smith, A.E.N. J. Inst. Met. 80, 477 (1952).
- [82] Smith, C.S. and Burns, J.W. J. Appl. Phys. 24, 15. 196 (1953).
- [83] Neighbours, J. and Smith, C.S. Acta Met. 2, 591, (1954).
- [84] Mizutani, U., Noguchi, S. and Massalski, T.B. Phys. Rev. 5, 2057, (1972).
- [85] White, G.K. Experimental techniques in low temperature Physics, (Oxford) 1968, p. 374.
- [86] Seitz, F. Modern theory of solids (McGraw-Hill) 1940, p. 110.
- [87] Keesom, P.H. and Pearlman, N. data compiled by in 'Introduction to solid state physics' by C.S. Kittel (John Wiley) 1956, 2nd Ed. p. 182.

- [88] deLaunay, J. Sol. St. Phys. (Ed.F.Seitz) V.2, 1956,  
p. 289.
- [89] Philips N.J. Phys. Rev. 114. 676 (1959).
- [90] Smithells, C.J. Metals Reference Book, (Butterworths)  
1967, p. 708.
- [91] Cottrell, A.H. An Introduction to Metallurgy (St. Martins)  
1967, p. 331.

## Appendix A

## DETAILED PROCEDURE FOR THE OPERATION OF THE ULTRASONIC EQUIPMENT

The operation of the ultrasonic equipment was started with the stabilization of the electronic systems. The 220 V power line of the electronic system was connected to the mains and the 'on-off' switch of the GR-1001-A Signal Generator was put at std.by. The 'Power - ON' switches of, P6-650-C R.F. pulsed amplifier and WA-600-E wide band amplifier were pressed to the ON - position. After about 5 minutes the 'High voltage ON' switch for the R.F. pulsed amplifier is pressed to the ON - position and the oscilloscope was put on. The system was then left for about 20 minutes for stabilization.

The 'OUTPUT' Knob of the Signal Generator was put at '2 VOLTS, over 400KC' position, 'METER' switch at the 'CARRIER' position. The 'CARRIER' Knob was adjusted to read 0.4 on the 'SET CARRIER' dial. The '2 VOLTS' output jack was connected to the 'GATED AMPLIFIER' jack of the pulsed amplifier. All connections were made by 93 ohms coaxial cables and Amphenol BNC jacks. The controls of the pulsed amplifier was set to the following : TRIGGER in INT (ernal) , PRF in maximum clockwise position, 'PULSE LENGTH' in 'LOCK' position, 'CW ACCESS' to CW, HV dial to 40 pct. and frequency to 10 MHz. Under

these conditions the pulsed output had a length of 105  $\mu$ sec, prf of 2.5 KHz, peak to peak voltage of 95 volts, carrier frequency of 10 MHz. The RF OUTPUT jack was then connected to the metal head of the specimen holder.

The specimen was then cleared and Dow corning 200 fluid was spread on one surface and the transducer placed on it. After clearing off extra fluid, the specimen was placed in the specimen holder. The GAIN Knob of the amplifier is then adjusted and the display on the CRO is stabilised by adjusting the operating Knobs of the oscilloscope. The time measurement was made as explained earlier in Chapter 2.

A 46608

Date Slip

This book is to be returned on the  
date last stamped.

.....	.....
.....	.....
.....	.....
.....	.....
.....	.....
.....	.....
.....	.....
.....	.....
.....	.....
.....	.....
.....	.....
.....	.....

CD 6.72.9

ME-1973-D-BAN-STU